ORIGINAL RESEARCH

Ecology and Evolution
Open Access WILEY

The complete mitochondrial genomes of two vent squat lobsters, *Munidopsis lauensis* and *M. verrilli*: Novel gene arrangements and phylogenetic implications

Shao'e Sun[1,2] | Zhongli Sha[1,2,3,4] (iD) | Yanrong Wang[1,2]

[1]Deep Sea Research Center, Institute of Oceanology, Chinese Academy of Science, Qingdao, China

[2]Center for Ocean Mega-Science, Chinese Academy of Sciences, Qingdao, China

[3]Laboratory for Marine Biology and Biotechnology, Qingdao National Laboratory for Marine Science and Technology, Qingdao, China

[4]University of Chinese Academy of Sciences, Beijing, China

Correspondence
Zhongli Sha, Deep Sea Research Center, Institute of Oceanology, Chinese Academy of Science, Qingdao 266071, China.
Email: shazl@qdio.ac.cn

Funding information
"Key Research Program of Frontier Sciences" of the Chinese Academy of Sciences, Grant/Award Number: QYZDB-SSWDQC036; China Postdoctoral Science Foundation, Grant/Award Number: 2018M630803; The Senior User Project of RV KEXUE, Grant/Award Number: KEXUE2017G10

Abstract

Hydrothermal vents are considered as one of the most extremely harsh environments on the Earth. In this study, the complete mitogenomes of hydrothermal vent squat lobsters, *Munidopsis lauensis* and *M. verrilli,* were determined through Illumina sequencing and compared with other available mitogenomes of anomurans. The mitogenomes of *M. lauensis* (17,483 bp) and *M. verrilli* (17,636 bp) are the largest among all Anomura mitogenomes, while the A+T contents of *M. lauensis* (62.40%) and *M. verrilli* (63.99%) are the lowest. The mitogenomes of *M. lauensis* and *M. verrilli* display novel gene arrangements, which might be the result of three tandem duplication–random loss (tdrl) events from the ancestral pancrustacean pattern. The mitochondrial gene orders of *M. lauensis* and *M. verrilli* shared the most similarities with *S. crosnieri.* The phylogenetic analyses based on both gene order data and nucleotide sequences (PCGs and rRNAs) revealed that the two species were closely related to *Shinkaia crosnieri.* Positive selection analysis revealed that eighteen residues in seven genes (*atp8, Cytb, nad3, nad4, nad4l, nad5, and nad6*) of the hydrothermal vent anomurans were positively selected sites.

KEYWORDS
adaptive evolution, Anomura, gene rearrangements, hydrothermal vent, mitochondrial genome

1 | INTRODUCTION

The Anomura MacLeay, 1838 is a highly diverse infraorder of decapod, including seven superfamilies, 17 families, and approximately 2,500 species (Ahyong, Schnabel, & Maas, 2009; Bracken-Grissom, Cannon, Cabezas, Feldmann, & Crandall, 2013; Schnabel, Ahyong, & Maas, 2011). The Galatheoidea are the most diverse superfamily within Anomura, with over 1,200 species placed in 69 genera, and have adapted to a wide range of habitats in freshwater, terrestrial, shallow-water coral reefs, and hydrothermal vent ecosystems (Baba

et al., 2008; De Grave et al., 2009). Deep-sea hydrothermal vent is one of the chemosynthetically driven ecosystems and characterized with high temperature (up to 390°C), low oxygen levels, enriched hydrogen sulfide (H2S), methane (CH4), and heavy metals, such as iron, zinc, and copper (Little & Vrijenhoek, 2003). Decapod crustaceans, such as alvinocaridid shrimps, bythograeid crabs, and galatheid squat lobsters, are dominant fauna in the hydrothermal vents, representing approximately 10% of all taxa reported from these vents (Little & Vrijenhoek, 2003; Martin & Haney, 2005; Yang et al., 2013). Recently, the hydrothermal vent bythograeid crabs (Hui, Song, Liu,

Li, & Cui, 2017) and alvinocaridid shrimps (Cottin et al., 2010; Hui, Cheng, & Sha, 2018; Wang et al., 2017; Zhang, Sun, Luan, Lian, & Sun, 2017) have demonstrated numerous genetic basis for the adaptations to vent habitats. However, little genomic and molecular genetic information are available for hydrothermal vent galatheid squat lobsters, impeding the study for the molecular mechanism in their adaptation process. A powerful system is needed to examine the adaptation evolution at the molecular level (e.g., mitochondrial genome).

The metazoan mitochondrial genome (mitogenome) is typically a circular double strand DNA molecule, encoding 13 protein-coding (PCG) genes (seven subunits of the NADH dehydrogenase complex, the cytochrome b subunit of the cytochrome bc1 complex, three subunits of the cytochrome c oxidase, and two subunits of ATP synthase), 22 transfer RNAs (tRNA) genes, two ribosomal RNAs (rRNA, *rrnS*, and *rrnL*) genes, and a control region (CR) including sites for the initiation of transcription and replication (Boore, 1999). Owing to its small genome size, higher evolutionary rates, limited recombination, and maternal inheritance, (Gissi, Iannelli, & Pesole, 2008; Simon, Buckley, Frati, Stewart, & Beckenbach, 2006), mitogenome has been widely used in species identification (Fu, Han, & Xiao, 2014; Kanmiya et al., 2011), molecular evolution (Cameron, 2014; Shao et al., 2015; Shao, Zhu, Barker, & Herd, 2012), phylogenetic relationship (Cameron, 2014; Cameron, Yoshizawa, Mizukoshi, Whiting, & Johnson, 2011; Chen, Wei, Shao, Dou, & Wang, 2014; Chen, Wei, Shao, Shi, et al., 2014), and population genetic (Wei et al., 2012; Zhang et al., 2014) studies. Although the gene content is relatively conservative, their rearrangements have been frequently reported, particularly in invertebrates at many taxonomic levels (Cameron, Johnson, & Whiting, 2007; Hassanin, Léger, & Deutsch, 2005). The gene rearrangement within a lineage has been supposed to be phylogenetically informative; therefore, comparative analysis of mitochondrial gene order has been proved to be a valuable phylogenetic tool (Akasaki et al., 2006; Boore & Brown, 1998; Smith, Arndt, Gorski, & Fajber, 1993; Yang, Ye, & Huang, 2016; Yuan, Li, Yu, & Kong, 2012). Based on the comparative analysis of mitochondrial gene arrangement, Smith et al. (1993) suggest that the sea cucumbers should group with sea urchins and sea stars with brittle stars. Akasaki et al. (2006) examined the mitochondrial gene arrangements of subclass Coleoidea and claimed that Octopoda showed the ancestral gene order, and the arrangements of mitochondrial genes in Oegopsida and Sepiida were derived from those of Octopoda. Based on the study of gene order rearrangements and phylogenetic relationships of five species belonging to Tellinoidea, Yuan et al. (2012) prefer to put the genus Sinonovacula within the superfamily Solenoidea instead of the superfamily Tellinoidea. Extensive mitochondrial gene rearrangements have been observed in crustaceans, such as copepods, anomuran, and brachyuran decapods, among which more frequent gene rearrangements exhibit compared with the putative ancestral gene order (Ki, Park, & Lee, 2009; Kim, Choi, Park, & Min, 2013; Machida, Miya, Nishida, & Nishida, 2002).

The 13 PCGs of mitogenome are all key subunits of complexes directly involved in the oxidative phosphorylation (OXPHOS)

process, directly providing 95% free energy for cells, which is important for metabolic demands in organisms (Gu et al., 2016; Wu, Gu, Guo, Huang, & Yang, 2016). In recent years, the mitogenome has become a powerful system for examining the genetic basis of organismal adaptation to various harsh environments, and signals of positive selection have been detected in mitochondrial genes of various taxa (Korkmaz, Aydemir, Temel, Budak, & Başıbüyük, 2017; Luo, Yang, & Gao, 2013; Scott et al., 2011; Wang et al., 2016; Yu, Wang, Ting, & Zhang, 2011; Yuan et al., 2018; Zhang et al., 2017; Zhou, Shen, Irwin, Shen, & Zhang, 2014). Most of these studies focused their attention on vertebrates, whereas few reports examined the adaptive evolution of crustacean mitogenomes to hydrothermal vent environments (Sun, Hui, Wang, & Sha, 2018; Wang et al., 2017). The molecular evolution of mitochondrial protein-coding genes in hydrothermal vent squat lobsters are still poorly understood. The mitogenome resources for the Anomura are limited to only ten mitogenomes as recorded on GenBank thus far, with five species from hydrothermal vents (http://blast.ncbi.nlm.nih.gov).

The *Munidopsis* is the second largest genus of galatheid squat lobsters, after *Munida*, with over 200 species, among which ten are endemic to the hydrothermal vent environments (Baba et al., 2008; Martin & Haney, 2005). In this study, we newly sequenced and annotated two complete mitogenomes of the hydrothermal vent squat lobsters, *M. lauensis* and *M. verrilli*. Combined with ten available anomuran mitogenomes, we performed a comparative mitogenomics analysis, in order to: (a) investigate the characteristics of Anomura mitogenomes; (b) assess the phylogenetic information of mitochondrial gene rearrangements; (c) rebuild a mitochondrial phylogeny of the Anomura that could be used as framework for further evolutionary studies; and (d) detect the signals of positive selection of mitochondrial genes in hydrothermal vent anomuran species during their adaptation to deep-sea hydrothermal vent environments.

2 | METHODS AND METHODS

2.1 | Sampling and DNA extraction

The hydrothermal vent squat lobsters, *M. lauensis* and *M. verrilli*, were captured from hydrothermal vent chimney at a depth of 1,121.5 m (119°17′08.321″E; 22°06′55.526″N) and 1,198.7 m (119°17′08.079″E; 22°06′55.432″N) in southwest Pacific Ocean, respectively. Both specimens were collected using the remotely operated vehicle (ROV) Quasar MkII of SMD in the United Kingdom, which was deployed using the RV KEXUE. They were immediately preserved in 95% ethanol after taken until DNA extraction. Total genomic DNA was extracted using the DNeasy tissue kit (Qiagen) accordingly.

2.2 | Illumina sequencing, genome assembly, and annotation

NEBNext® Ultra™ DNA Library Prep Kit for Illumina (NEB) was used to generate the sequencing libraries following manufacturer's

instructions. And then, the index codes were added to attribute sequences to the sample. The clustering of the index-coded sample was performed on a cBot Cluster Generation System. Sequencing was performed based on an Illumina HiSeq 2500 platform, with the paired-end reads generated for each sample. The paired-end raw reads were filtered, and the reads with average quality value lower than Q20 were excluded from further analysis (Sun, Hui, Wang, et al., 2018; Sun, Sha, & Wang, 2018a). CLC Genomics Workbench v. 11.0.64 (http://www.clcbio.com/products/clcgenomics-workbench/) and SOAP denovo (k-mer = 55) (Li et al., 2010) were selected to assemble the clean data. De novo assembled contigs longer than 10 Kbp were blasted against the NCBI nr database using the "BLAST" tool implemented in the CLC Genomics Workbench to extract the "mitochondrial DNA" contigs. The cutoff E-value of 1.0E-15 was used. In order to identify contigs of mitochondrial origin, we aligned the putative mtDNAs of *M. lauensis* and *M. verrilli* with the published complete mitochondrial genomes of the Galatheoidea, *Kiwa tyleri* (KY423514), *Munida gregaria* (KU521508), *Neopetrolisthes maculatus* (KC107816), *Shinkaia crosnieri* (EU420129), and *Petrolisthes haswelli* (LN624374) with the aid of "Alignment" tool implemented in the CLC Genomic Workbench with the default setting. In order to establish a circular mitochondrial DNA (mtDNA), the contigs identified as mitogenome sequences were manually checked for overlap at the beginning and end of the sequence. To evaluate the average sequence coverage of mitochondrial genomes, we mapped sequences against the assembled mitochondrial genomes using GNUMAP (Clement et al., 2010).

The protein-coding genes were searched by ORF Finder (http://www.ncbi.nlm.nih.gov/gorf/gorf.html), BLASTx, and MITOS Web Server (Bernt et al., 2013) using the invertebrate mitochondrial genetic code. The sequences and positions of tRNA genes were determined by ARWEN (Laslett & Canback, 2008) and MITOS Web Server (Bernt et al., 2013) with the default search mode. The rRNA genes were identified by blasting the inferred sequences against to other published crustacean mtDNA sequences (http://www.ncbi.nlm.nih.gov/BLAST). The gene maps of the *M. lauensis* and *M. verrilli* mitogenomes were drawn with the program CGView (Stothard & Wishart, 2005). The complete mtDNA sequences of *M. lauensis* and *M. verrilli* have been deposited in the GenBank database with the accession numbers MH717895 and MH717896, respectively.

2.3 | Sequence analysis

The relative synonymous codon usage (RSCU) values and nucleotide composition were calculated using MEGA 5 (Tamura et al., 2011). The GC and AT-skew values were obtained according to the formulae by Perna and Kocher (1995): AT-skew = (A−T)/(A+T); GC-skew = (G−C)/(G+C), where A, T, G, and C are the occurrences of the four nucleotides. DnaSP5.1 (Librado & Rozas, 2009) was taken to determine the effective number of codons (ENC) and the codon bias index (CBI) for each PCG. Tandem Repeats Finder 4.0 (Benson, 1999) was used to search the tandem repeat sequences, and the potential secondary structures of the repeat sequences were predicted by Mfold

software version 3.2 (Zuker, 2003). When more than one secondary structures were detected, the most stable one with lowest free energy $\triangle G$ was selected.

2.4 | Build phylogeny from gene order data

Along with mitogenome sequences of *M. lauensis* and *M. verrilli* (this study), other 10 available mitogenomes from Anomura, including *Paralithodes brevipes* (AB735677), *Petrolisthes haswelli* (LN624374), *Pagurus longicarpus* (AF150756), *Paralithodes camtschaticus* (JX944381), *Lithodes nintokuae* (AB769476), *Clibanarius infraspinatus* (LN626968), *K. tyleri* (KY423514), *M. gregaria* (KU521508), *N. maculatus* (KC107816), and *S. crosnieri* (EU420129), were used in gene order comparison. CREx (Bernt et al., 2007) was used to conduct pairwise comparisons of the mitochondrial gene order. CREx inferred the most possible scenarios for gene rearrangements based on common intervals. MLGO web server (http://www.geneorder.org/server.php; Hu, Lin, & Tang, 2014; Zhou, Lin, Feng, Zhao, & Tang, 2017) was used to infer a phylogeny from gene order data.

2.5 | Build phylogeny from nucleotide sequences

Neighbor-joining (NJ) tree based on uncorrected *p* distances among mitochondrial tRNA genes from 12 Anomura taxa (described above) was constructed using MEGA 5 (Tamura et al., 2011). Maximum likelihood (ML) and Bayesian inference (BI) were employed for phylogenetic reconstructions of the 12 Anomura species based on nucleotide sequences of 13 PCGs and 2 rRNA genes using 14 species from five other decapod infraorders (Table S1) as outgroup taxa. The nucleotide sequences for the PCG and rRNA genes were aligned with MAFFT version 6 online (http://mafft.cbrc.jp/alignment/software/), applying the E-INS-I manual strategy with default parameters. Areas of dubious alignment were recognized by the program Gblocks (Talavera & Castresana, 2007) (default setting) and excluded from the analyses. PartitionFinder v1.1.1 (Lanfear, Calcott, Ho, & Guindon, 2012) was used to determine the best partitioning schemes and corresponding substitution models. The data blocks were predefined by genes and codon positions for nucleotide sequences of protein-coding genes. The Bayesian information criterion (BIC) and the greedy heuristic search algorithm with branch lengths were estimated as "unlinked" to identify the best-fit partition schemes. The best-fit partitioning schemes (Table S2) were adopted in the phylogenetic analyses.

Maximum likelihood was employed in RAxML Black-Box web-server (http://phylobench.vital-it.ch/raxml-bb/index.php; Stamatakis, Hoover, & Rougemont, 2008). Bootstrap (BP) values were determined using 1,000 bootstrap replicates. BI analysis was performed by MrBayes 3.1 software (Ronquist & Huelsenbeck, 2003). The Markov chain Monte Carlo (MCMC) was run for 10,000,000 generations (sampling every 1,000 generations) to allow adequate time for convergence. When the standard deviation of split frequencies was <0.01, the run was stopped. All parameters were checked with Tracer v 1.5 (Drummond & Rambaut, 2007). After omitting the first 5,000

"burn in" trees, the remaining 5,000 sampled trees were selected to estimate the 50% majority rule consensus tree and the Bayesian posterior probabilities (PP).

2.6 | Determine the signals of selection

The codon-based likelihood approach implemented in the CODEML program from PAML (Yang, 2007) was used to evaluate the potential selective pressures in the mitochondrial PCGs of hydrothermal vent anomurans. The 13 individual PCGs and the concatenated dataset were involved in the positive selection analysis. The tree topologies inferred from tree-building methods in the present study were used. The ratio of nonsynonymous to synonymous substitution rates (Ka/Ks, denoted ω) was taken as a measure of selective pressure. The signals of selection were assessed under several models: one-ratio model (M0), free-ratio model (M1), and two-ratio model (M2). To identify the probabilities of specific residues under positive selection in each gene of the hydrothermal vent anomurans species (marked as foreground branch), the branch-site Model A (positive selection model) was selected, which allowed ω to vary across lineages and sites. All the positively selected sites were determined by Bayes empirical Bayes (BEB) method (Yang, Wong, & Nielsen, 2005) with posterior probabilities of ≥0.95.

3 | RESULTS AND DISCUSSION

3.1 | De novo assemblies of *M. lauensis* and *M. verrilli* mitogenomes

The Hiseq runs resulted in 33,862,831 (10.16 G) and 46,095,676 (13.83 G) paired-end clean reads from *M. lauensis* and *M. verrilli*

libraries, respectively. The sequencing qualities were generally high for both squat lobsters. About 93.77% of the reads in *M. lauensis* and 90.54% of the reads in *M. verrilli* passed Q20, indicating the probability of a base call error ≤0.01. There were in total 425,589 and 579,932 contigs assembled de novo based on the paired-end reads for *M. lauensis* and *M. verrilli*, respectively. The lengths of most contigs (82.1% and 85.3% in *M. lauensis* and *M. verrilli*, respectively) were <1 Kbp. Only eleven *M. lauensis* contigs and thirteen *M. verrilli* contig had lengths longer than 10 Kbp. The average sequence coverage was 11.0 and 13.0 for all the assembled contigs of *M. lauensis* and *M. verrilli*. The blast results suggested that the top hits (E-value = 0) of the longest contig in each sample (17,520 and 17,659 bp for *M. lauensis* and *M. verrilli*, respectively) were the mitogenomes of Galatheoidea species. Therefore, there was a highly possibility that the longest contig in each sample was the mitogenome of *M. lauensis* or *M. verrilli*, which was assembled from multiple overlapping reads. A total of 29,861 (*M. lauensis*) and 40,648 (*M. verrilli*) multiple overlapping reads were mapped onto the longest mitochondrial contigs, giving an average coverage 511× for *M. lauensis* and 691× for *M. verrilli* mtDNAs, which were about 46–53 times higher than that of all contigs. The higher sequencing coverage of mtDNAs is consistent with the high copy numbers of mitochondria in eukaryotic cells and indirectly confirm the mitochondrial origin of the sequences (Hung et al., 2013).

3.2 | General genome characteristics

The complete mitogenomes of *M. lauensis* and *M. verrilli* were 17,483 bp and 17,636 bp in length, respectively (Figure 1, Table 1). The sizes of both mitogenomes are the largest among the length range of all available Anomura mitogenomes (approximately
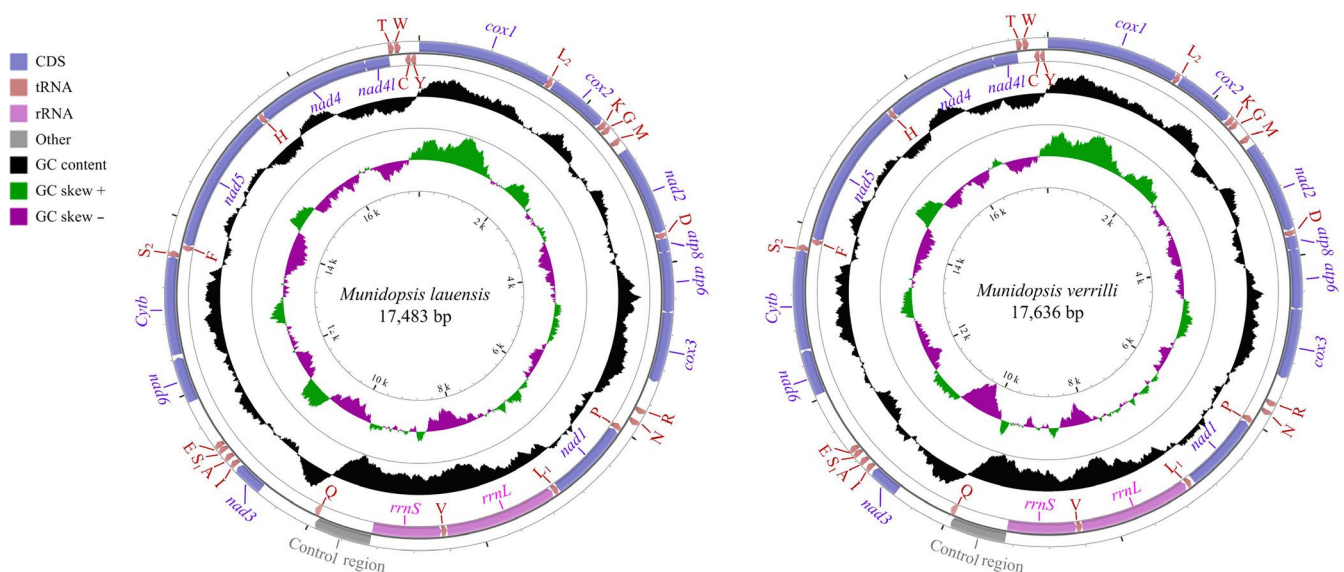
FIGURE 1 The organization of the mitogenomes of *Munidopsis lauensis and M. verrilli*. The full names of protein-coding genes, *rrnS* and *rrnL*, are listed under abbreviations. *rrnS* and *rrnL*, 12S and 16S ribosomal RNA genes, respectively; *atp6* and *atp8*, ATPase subunit 6 and 8 genes, respectively; *cox1-cox3*, cytochrome c oxidase subunits I-III genes, respectively; *cytb*, cytochrome b gene; *nad1-6* and *4l*, NADH dehydrogenase subunit 1–6 and 4 L genes, respectively. One uppercase letter amino acid abbreviations are used to label the corresponding tRNA genes

TABLE 1 Organization of the mitogenomes of *Munidopsis lauensis* and *M. verrilli*

Feature	Position Ml (Intergenic nucleotides)[a]	Position Mv (Intergenic nucleotides)[a]	Length (stop codon included) Ml	Length (stop codon included) Mv	Start codon Ml	Start codon Mv	Stop codon Ml	Stop codon Mv	Anticodon	Strand
cox1	1–1,503 (−6)	1–1,503 (−4)	1,503	1,503	ATT	ATT	TAA	TAA		+
trnL2	1,498–1,566 (6)	1,500–1,564 (8)	69	65					TAA	+
cox2	1,573–2,253 (8)	1,573–2,253 (11)	681	681	ATG	ATG	TAA	TAA		+
trnK	2,262–2,331 (2)	2,265–2,333 (2)	70	69					TTT	+
trnG	2,334–2,396 (103)	2,336–2,398 (138)	63	63					TCC	+
trnM	2,500–2,567 (87)	2,537–2,604 (61)	68	68					CAT	+
nad2	2,655–3,659 (6)	2,666–3,703 (6)	1,005	1,038	ATT	ATT	TAA	TAA		+
trnD	3,666–3,732 (0)	3,710–3,777 (0)	67	68					GTC	+
atp8	3,733–3,891 (−7)	3,778–3,936 (−7)	159	159	GTG	GTG	TAA	TAA		+
atp6	3,885–4,559 (−1)	3,930–4,604 (−1)	675	675	ATG	ATG	TAA	TAA		+
cox3	4,559–5,350 (326)	4,604–5,395 (281)	792	792	ATG	ATG	TAA	TAA		+
trnR	5,677–5,744 (74)	5,677–5,743 (45)	68	67					TCG	+
trnN	5,819–5,884 (69)	5,789–5,854 (95)	66	66					GTT	+
trnP	5,954–6,026 (8)	5,950–6,022 (9)	73	73					TGG	−
nad1	6,035–7,000 (2)	6,032–6,973 (26)	966	942	GTG	GTG	TAG	TAA		−
trnL1	7,003–7,070 (8)	7,000–7,065 (11)	68	66					TAG	−
rrnL	7,079–8,410 (2)	7,077–8,409 (0)	1,332	1,333						−
trnV	8,413–8,478 (0)	8,410–8,475 (−1)	66	66					TAC	−
rrnS	8,479–9,291 (0)	8,475–9,297 (0)	813	823						−
CR	9,292–9,941 (0)	9,298–9,944 (0)	650	647						−
trnQ	9,942–10,008 (644)	9,945–10,011 (628)	67	67					TTG	+
nad3	10,653–11,006 (26)	10,640–10,993 (24)	354	354	ATT	ATT	TAA	TAA		+
trnI	11,033–11,099 (30)	11,018–11,084 (32)	67	67					GAT	+
trnA	11,130–11,196 (40)	11,117–11,184 (42)	67	68					TGC	+
trnS1	11,237–11,301 (0)	11,227–11,291 (0)	65	65					TCT	+
trnE	11,302–11,370 (531)	11,292–11,359 (691)	69	68					TTC	+
nad6	11,902–12,417 (32)	12,051–12,566 (11)	516	516	ATC	ATC	TAA	TAA		+
cytb	12,450–13,554 (−4)	12,578–13,703 (−3)	1,105	1,126	ATT	ATC	T - -	T - -		+
trnS2	13,551–13,621 (16)	13,701–13,769 (15)	71	69					TGA	−

(Continues)

TABLE 1 (Continued)

Feature	Position		Length (stop codon included)		Start codon		Stop codon		Anticodon	Strand
	MI (Intergenic nucleotides)[a]	Mv (Intergenic nucleotides)[a]	MI	Mv	MI	Mv	MI	Mv		
trnF	13,638–13,701 (1)	13,785–13,848 (−3)	64	64					GAA	−
nad5	13,702–15,430 (0)	13,846–15,577 (0)	1,729	1,732	ATG	ATG	T - -	T - -		−
trnH	15,431–15,498 (−1)	15,578–15,643 (−2)	68	66					GTG	−
nad4	15,498–16,837 (−7)	15,643–16,982 (−7)	1,340	1,340	ATG	ATG	TA -	TA -		−
nad4l	16,831–17,133 (1)	16,976–17,278 (1)	303	303	ATG	ATG	TAA	TAA		+
trnT	17,135–17,202 (5)	17,280–17,347 (5)	68	68					TGT	+
trnW	17,208–17,277 (39)	17,353–17,422 (49)	70	70					TCA	−
trnC	17,317–17,381 (−1)	17,472–17,536 (0)	65	65					GCA	−
trnY	17,381–17,445 (38)	17,537–17,599 (37)	65	63					GTA	−

[a]Intergenic regions refer to noncoding bases between the feature on the same line and the feature on the above line, with a negative number indicating an overlap.

16,000 bp). The plausible explanation for this phenomenon may be the extension of noncoding regions, which were 2,077 and 2,200 bp in *M. lauensis* and *M. verrilli*, respectively. Each genome contained the typical 13 PCGs, 22 tRNA genes, 2 rRNA genes, and one control region (CR). Within these genes, 9 PCGs and 14 tRNAs were encoded by the light strand, while 4 PCGs, 8 tRNAs, and 2 rRNAs were encoded by the minority strand. Considering their location and AT-richness, we supposed continuous region between *rrnS* and *trnQ* to be the CR as in the case of the hydrothermal vent galatheid crab *S. crosnieri* (Yang & Yang, 2008). The overlapping nucleotides from seven adjacent genes in the mitogenome of *M. lauensis* were discovered up to 27 bp in total. In the case of *M. verrilli* mitogenome, eight overlaps between adjacent genes were up to 28 bp.

The base composition (A+T content, G+C content) and strand asymmetry (AT-skew, GC-skew) were usually used to investigate the nucleotide-compositional behavior of mitogenomes (Hassanin et al., 2005). The nucleotide compositions of the complete mtDNA sequence for *M. lauensis* and *M. verrilli* were both biased toward A and T (Table 2). The A+T content was 62.40% in *M. lauensis* and 63.99% in *M. verrilli*, which were the lowest among the available Anomura mitogenomes. The lowest A+T content was also found in the PCGs, tRNAs, and rRNAs (Table 2). In order to further evaluate the base bias in the mitogenomes, we measured skewness in different gene regions of *M. lauensis* and *M. verrilli* mitogenomes, and found the whole genomes of the hydrothermal vent squat lobsters were all positively AT-skewed (0.086 and 0.077) and negatively GC-skewed (−0.336 and −0.363). The AT-skew and GC-skew of the two mitogenomes were all stronger than those of the other anomurans (Table 2).

3.3 | Protein-coding genes and codon usage

In the mitogenomes of *M. lauensis* and *M. verrilli*, the region of PCGs was 11,128 and 11,161 bp in size (stop codon included), respectively. And the overall A+T content of the 13 PCGs was 60.16 (*M. lauensis*) and 61.64% (*M. verrilli*), which were lower than those of other anomurans. The AT-skew and GC-skew of the PCGs in both mitogenomes were negative (Table 2). In the mitogenomes of *M. lauensis* and *M. verrilli*, 11 PCGs began with the standard ATN start codon. The codon GTG was found to be the initiator codon for the *atp8* and *nad1* genes. Ten PCGs ended with complete stop codon TAA, whereas the *nad4* gene was terminated by incomplete stop codon TA, and *cytb* and *nad5* were terminated by a single T. The presence of incomplete stop codons is common phenomenon in invertebrate mitochondrial genes, which is presumably completed as TAA via post-transcriptional polyadenylation (Cannicci et al., 2017; Ivey & Santos, 2007; Ojala, Montoya, & Attardi, 1981).

The RSCU values for the 13 PCGs were summarized in Table 3. The *M. lauensis* and *M. verrilli* mitogenomes encoded 3,699 and 3,710 amino acids, respectively. The amino acids Ser (RSCU = 2.19), Leu (RSCU = 2.14), and Phe (RSCU = 1.62) were mostly used in *M. lauensis* mitogenome. Also in *M. verrilli* mitogenome, Ser (RSCU = 2.20), Leu (RSCU = 2.07), and Phe (RSCU = 1.55) were the most common

TABLE 2 Genomic features of the mitogenomes of Anomura species

Species	Genome Length (bp)	AT%	AT-Skew	GC-Skew	13 Protein-coding genes AT%	AT-Skew	GC-Skew	rRNAs AT%	AT-Skew	GC-Skew	tRNAs AT%	AT-Skew	GC-Skew	Control region AT%	AT-Skew	GC-Skew
Paralithodes camtschaticus	16,720	73.86	0.003	−0.132	71.57	−0.168	0.014	77.98	0.038	0.238	75.12	0.008	0.146	–	–	–
Lithodes nintokuae	15,731	73.28	−0.003	−0.127	71.28	−0.176	0.031	77.97	0.041	0.235	76.78	0.024	0.110	–	–	–
Paralithodes brevipes	16,303	72.50	0.009	−0.134	70.23	−0.173	0.034	77.42	0.039	0.240	75.99	0.020	0.156	–	–	–
Petrolisthes haswelli	15,348	70.01	−0.019	−0.244	68.61	−0.194	−0.011	73.18	0.035	0.302	72.15	−0.015	0.136	76.45	−0.041	−0.324
Pagurus longicarpus	15,630	71.28	0.029	−0.213	69.61	−0.170	−0.013	77.15	0.011	0.310	73.17	0.024	0.126	–	–	–
Clibanarius infraspinatus	16,504	67.94	0.042	−0.199	66.37	−0.193	0.037	71.18	−0.050	0.322	70.62	0.001	0.142	69.47	−0.023	−0.118
Neopetrolisthes maculatus	15,324	71.26	−0.020	−0.210	70.13	−0.185	−0.005	74.71	0.080	0.294	72.71	0.011	0.091	75.14	0.002	−0.118
Kiwa tyleri	16,865	79.32	−0.044	−0.220	76.18	−0.176	0.005	83.64	0.067	0.039	78.92	0.030	0.062	–	–	–
Munida gregaria	16,326	74.94	−0.020	−0.162	72.47	−0.196	0.051	79.26	−0.015	0.335	76.12	0.001	0.140	84.95	−0.013	−0.131
Shinkaia crosnieri	15,182	72.88	−0.014	−0.313	70.96	−0.184	−0.025	77.92	0.045	0.336	74.46	0.006	0.121	83.49	−0.158	−0.741
Munidopsis lauensis	17,483	62.40	0.086	−0.336	60.13	−0.180	−0.034	70.49	−0.015	0.384	69.59	0.023	−0.224	73.38	0.392	−0.283
Munidopsis verrilli	17,636	63.99	0.077	−0.363	61.64	−0.184	−0.039	70.83	0.002	0.386	69.25	0.020	−0.236	75.27	0.228	−0.313

amino acids. RSCU also reflects a nucleotide composition bias in *M. lauensis* and *M. verrilli* mitogenomes. The RSCU values for the codons NNU and NNA were usually higher than 1, suggesting a strong A+T-bias in their third codon position (Table 3). This result supports the hypothesis that there should be a positive correlation between the codon usage bias and the AT bias of the third codon position for the mitogenomes (Chai, Du, & Zhai, 2012; Hao et al., 2012; Kim et al., 2009; Salvato, Simonato, Battisti, & Negrisolo, 2008).

In order to further explore the codon usage bias among anomuran species, we analyzed the correlations between the effective number of codons (ENC), codon bias index (CBI), the G+C content of all codons (G+Cc), and the G+C content of the third codon position (G+C3s). We found ENC and CBI (R^2 = .997), CBI and G+Cc (R^2 = .984), and CBI and G+C3s (R^2 = .827) were negatively related, whereas ENC and G+Cc (R^2 = .978), and ENC and G+C3s (R^2 = .971) were positively related (Figure 2). These results are in consistent with the neutral mutational theories that the codon usage bias among organisms are mostly determined by the G+C content of the mitogenomes (Chen, Lee, Hottes, Shapiro, & McAdams, 2004; Plotkin & Kudla, 2011).

3.4 | Transfer and ribosomal RNA genes

The complete set of 22 tRNA genes, typical of metazoan mitogenomes (two for each of serine and leucine, and one for each of the other 18 amino acids), were identified from in *M. lauensis* and *M. verrilli* mitogenomes. The tRNA genes ranged from 63 bp (*trnG*, as well as *trnY* in *M. verrilli* mitogenome) to 73 bp (*trnP*) in size and showed a strong A+T bias (69.59% and 69.25% in *M. lauensis* and *M. verrilli*, respectively). The AT-skews were positive and GC-skew were negative for the tRNA genes in both mitogenomes. Almost all of the tRNAs could be folded into a typical clover-leaf secondary structures containing four functional arms and corresponding loops (Figures S1 and S2). However, *trnS1* had no dihydrouridine (DHU) arm in the secondary structure. Although the tRNA content was conserved in *Munidopsis* mitogenomes, their arrangement was specific (see Section 3.5). The tRNA gene rearrangement in mitochondrial genomes can probably be explained by tandem duplication mechanism and tRNA gene recruitment (Dowton & Austin, 1999; Wang & Lavrov, 2011). In order to explore the possible evolutionary mechanism of tRNA gene rearrangement in *Munidopsis* mitogenomes, we analyzed tRNA gene sequences from 12 Anomura mitogenomes. The NJ tree showed that the equivalent tRNA genes (with the same amino acid and anticodon identities) from different species form well-defined clades (Figure 3). This result revealed the orthologous relationships of each equivalent tRNAs. Thus, the tRNA gene rearrangement in *Munidopsis*, and even other anomuran mitogenomes, most probably arises from tandem duplication and random loss of tRNA genes, instead of tRNA gene recruitment.

The *rrnL* genes were located between *trnL1* and *trnV*, while *rrnS* were located between *trnV* and CR (Figure 1 and Table 1). In *M. lauensis* and *M. verrilli* mitogenomes, the A+T content of the two

TABLE 3 Codon usage of *Munidopsis lauensis* (Ml) and *M. verrilli* (Mv) PCGs

Amino acid	Codon	Ml N (RSCU)[a]	Mv N (RSCU)[a]	Amino acid	Codon	Ml N (RSCU)[a]	Mv N (RSCU)[a]
F	UUU	261 (1.62)	260 (1.55)	Y	UAU	63 (1.00)	70 (1.12)
	UUC	62 (0.38)	75 (0.45)		UAC	63 (1.00)	55 (0.88)
L	UUA	206 (2.14)	211 (2.07)	H	CAU	14 (0.33)	29 (0.69)
	UUG	109 (1.13)	108 (1.06)		CAC	70 (1.67)	55 (1.31)
L	CUU	82 (0.85)	97 (0.95)	Q	CAA	55 (1.49)	61 (1.65)
	CUC	56 (0.58)	73 (0.72)		CAG	19 (0.51)	13 (0.35)
	CUA	99 (1.03)	98 (0.96)	N	AAU	62 (0.89)	80 (1.18)
	CUG	26 (0.27)	24 (0.24)		AAC	78 (1.11)	56 (0.82)
I	AUU	185 (1.34)	197 (1.34)	K	AAA	57 (1.31)	64 (1.35)
	AUC	92 (0.66)	97 (0.66)		AAG	30 (0.69)	31 (0.65)
M	AUA	104 (1.30)	116 (1.27)	D	GAU	28 (0.80)	27 (0.93)
	AUG	56 (0.70)	66 (0.73)		GAC	42 (1.20)	31 (1.07)
V	GUU	89 (1.30)	96 (1.51)	E	GAA	53 (1.15)	46 (1.06)
	GUC	35 (0.51)	27 (0.43)		GAG	39 (0.85)	41 (0.94)
	GUA	70 (1.02)	64 (1.01)	C	UGU	27 (1.15)	28 (1.22)
	GUG	80 (1.17)	67 (1.06)		UGC	20 (0.85)	18 (0.78)
S	UCU	93 (2.19)	99 (2.20)	W	UGA	56 (1.18)	60 (1.24)
	UCC	28 (0.66)	43 (0.96)		UGG	39 (0.82)	37 (0.76)
	UCA	48 (1.13)	49 (1.09)	R	CGU	10 (0.66)	12 (0.80)
	UCG	9 (0.21)	11 (0.24)		CGC	11 (0.72)	6 (0.40)
P	CCU	37 (1.00)	41 (1.12)		CGA	31 (2.03)	30 (2.00)
	CCC	59 (1.59)	54 (1.47)		CGG	9 (0.59)	12 (0.80)
	CCA	36 (0.97)	41 (1.12)	S	AGU	23 (0.54)	32 (0.71)
	CCG	16 (0.43)	11 (0.30)		AGC	35 (0.82)	20 (0.44)
T	ACU	43 (1.00)	62 (1.27)		AGA	40 (0.94)	56 (1.24)
	ACC	65 (1.51)	60 (1.23)		AGG	64 (1.51)	50 (1.11)
	ACA	54 (1.26)	57 (1.17)	G	GGU	47 (0.80)	44 (0.75)
	ACG	10 (0.23)	16 (0.33)		GGC	46 (0.79)	36 (0.61)
A	GCU	93 (1.56)	87 (1.47)		GGA	52 (0.89)	76 (1.29)
	GCC	77 (1.29)	75 (1.27)		GGG	89 (1.52)	79 (1.34)
	GCA	47 (0.79)	53 (0.90)				
	GCG	22 (0.37)	21 (0.36)				

Note: N: number of occurrence of the codon; RSCU, relative synonymous codon usage.
[a]The value in the brackets refer to the RSCU.

rRNA genes were 70.49% and 70.83%, respectively, which were the lowest among anomuran species (Table 2). The AT-skew of the two rRNAs was negative (−0.015) in *M. lauensis*, while it was positive (0.002) in *M. verrilli*. The GC-skew in both species were positive (0.384 and 0.386, respectively).

3.5 | Control region

Twenty-six noncoding regions, totaling 2,754 bp, were interspersed throughout the *M. lauensis* mitogenome, while the corresponding values were 24 and 2,875 bp in *M. verrilli*. The noncoding regions located between *rrnS* and *trnQ* (650 and 647 bp in *M. lauensis* and *M. verrilli*, respectively) corresponds to the CR identified in other decapods, which may contain the signals for replication and transcription (Taanman, 1999). The A+T content of the predicted control region in *M. lauensis* and *M. verrilli* was 73.38% and 75.27%, respectively, with both negative AT-skew (0.392 and 0.228) and positive GC-skew (−0.283 and −0.313). In the CR of *M. lauensis* mitogenome, one 205-bp tandem repeat region (9,723–9,927) was found, which comprised three nearly identical motifs with 70, 71, and 64 bp in length, respectively (Figure 4). The CR of *M. verrilli* contained a 174-bp repeat sequence (9,518–9,691),
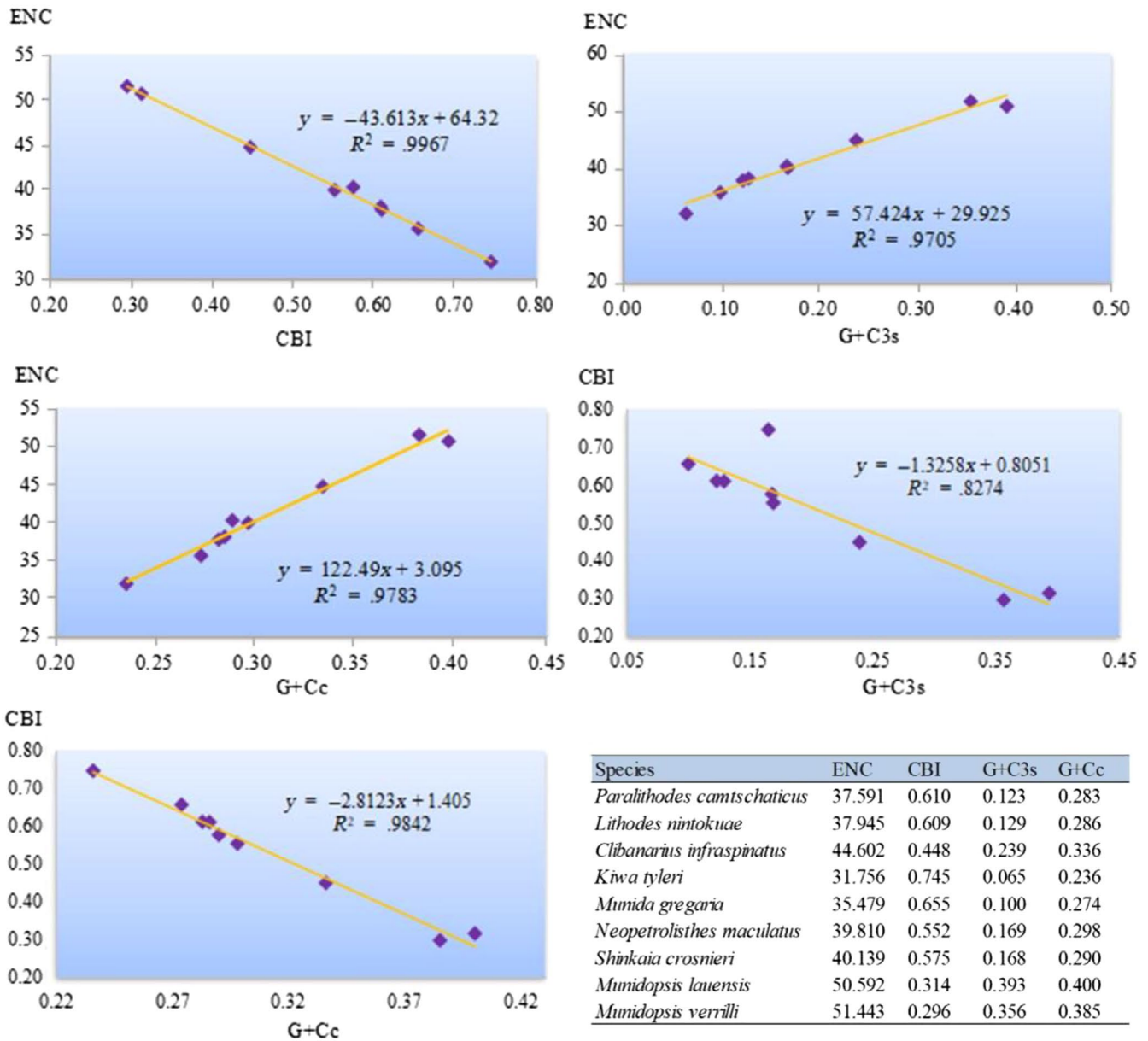
Species	ENC	CBI	G+C3s	G+Cc
Paralithodes camtschaticus	37.591	0.610	0.123	0.283
Lithodes nintokuae	37.945	0.609	0.129	0.286
Clibanarius infraspinatus	44.602	0.448	0.239	0.336
Kiwa tyleri	31.756	0.745	0.065	0.236
Munida gregaria	35.479	0.655	0.100	0.274
Neopetrolisthes maculatus	39.810	0.552	0.169	0.298
Shinkaia crosnieri	40.139	0.575	0.168	0.290
Munidopsis lauensis	50.592	0.314	0.393	0.400
Munidopsis verrilli	51.443	0.296	0.356	0.385

FIGURE 2 Evaluation of codon bias in the mitogenomes of twelve anomuran species. ENC, effective number of codons; CBI, codon bias index; G+Cc, G+C content of all codon positions; G+C3s, G+C content of the third codon positions

which included two nearly identical motifs (Figure 4). The slipped-strand mispairing during mtDNA replication may result in the occurrence of tandem repeats (Levinson & Gutman, 1987). Each tandem repeat motif could be folded into stem-loop secondary structures (Figure 4), which may play an important part in mtDNA duplications (Stanton, Daehler, Moritz, & Brown, 1994; Wilkinson & Chapman, 1991). Additionally, special "G(A)$_n$T" motif and AT-rich sequences were also observed in the CRs of *M. lauensis* and *M. verrilli*. Similar characteristics were also reported in the deep-sea anemone *Bolocera* sp. (Zhang, Zhang, Wang, Zhang, & Lin, 2017), deep-sea spongicolid shrimp *Spongiocaris panglao* (Sun et al., 2018a), and the hydrothermal vent alvinocaridid shrimp *Shinkaicaris leurokolos* (Sun, Hui, Wang, et al., 2018).

3.6 | Mitochondrial gene order and rearrangements

The *M. lauensis* and *M. verrilli* showed a novel arrangement of mitochondrial genes (Figure 5). Their gene order diverged in many positions from that of the ancestral pancrustacean pattern, which is shared by lots of crustaceans and hexapods (Boore, Lavrov, & Brown, 1998). Totally, we identified at least ten rearrangements in *M. lauensis* and *M. verrilli* mitogenomes compared with the ancestral pancrustacean pattern (Figure 5). The main rearrangements were tRNA translocations, and four rearrangements involved in PCGs. One of the major fragment containing *trnF*, *nad5*, *trnH*, *nad4*, *nad4l*, and *trnT* moved to downstream of *trnS$_2$* from its ancestral position; the other major fragment containing *nad1*, *trnL$_1$*, *rrnL*,
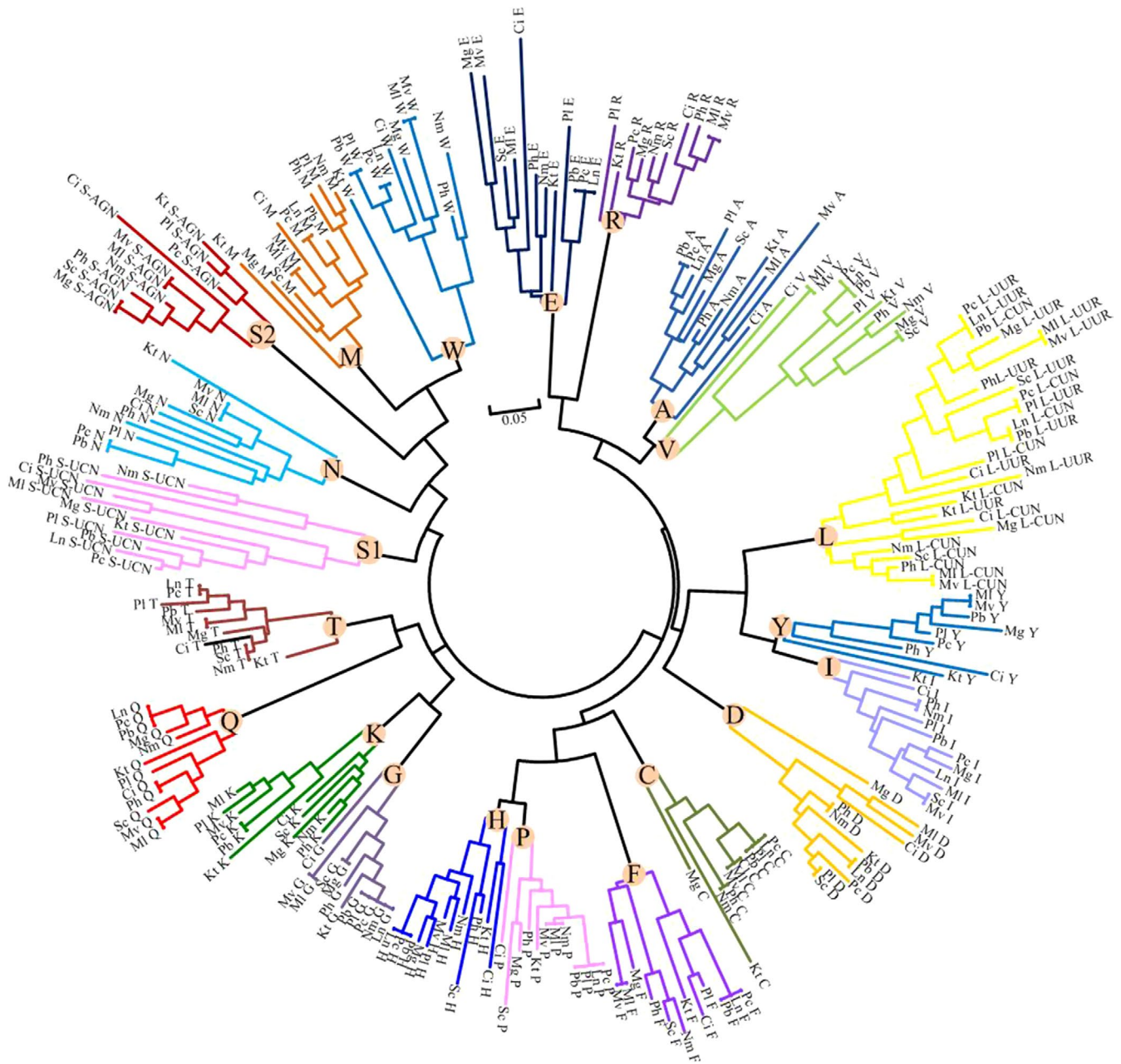
FIGURE 3 Neighbor-joining tree based on uncorrected *p* distances among mitochondrial tRNA genes from twelve anomuran species. Pb, *Paralithodes brevipes*; Ph, *Petrolisthes haswelli*; Pl, *Pagurus longicarpus*; Pc, *Paralithodes camtschaticus*; Ln, *Lithodes nintokuae*; Ci, *Clibanarius infraspinatus*; Kt, *Kiwa tyleri*; Mg, *Munida gregaria*; Nm, *Neopetrolisthes maculatus*; Sc, *Shinkaia crosnieri*; Ml, *Munidopsis lauensis*; and Mv, *Munidopsis verrilli*

trnV, *rrnS*, and CR moved to downstream of *trnN*. The *nad3* gene, located between *trnG* and *trnA*, translocated to the position between *trnQ* and *trnI*. And the fraction *trnM-nad2* was located between *trnG* and *trnD* instead of the original position between *trnQ* and *trnW* genes. The *trnG*, *trnA*, *trnP*, *trnQ* moved to upstream of *trnM*, *trnS₁*, *nad1*, *nad3*, respectively. The *trnI* moved to the downstream of *nad3* gene. The gene block *trnS1-trnE* translocated to the middle of *trnA* and *nad6*. According to the CREx analyses, these novel gene orders of *M. lauensis* and *M. verrilli* might be the result of 3 tandem duplication–random loss (tdrl) events from the ancestral pancrustacean pattern (Figure S3).

The twelve anomurans exhibited nine types of gene organization, which differ from any gene order ever reported in decapods. *P. haswelli*, *M. gregaria*, and *N. maculatus* showed the most similarities in mitochondrial gene order with the ancestral pancrustacean pattern (Figure 6). The mitochondrial gene orders of *M. lauensis* and *M. verrilli* (Type I in Figure 5) shared the most similarities with *S. crosnieri* (Type II). This result was consistent with previous study (Yang & Yang, 2008). *K. tyleri* (Type III) shared higher similarities with Type IV (*P. haswelli/M. gregaria/N. maculatus*. These results are consistent with the conclusion from the gene order-based phylogenetic tree (Figure 5). *M. lauensis* and *M. verrilli* showed a closest
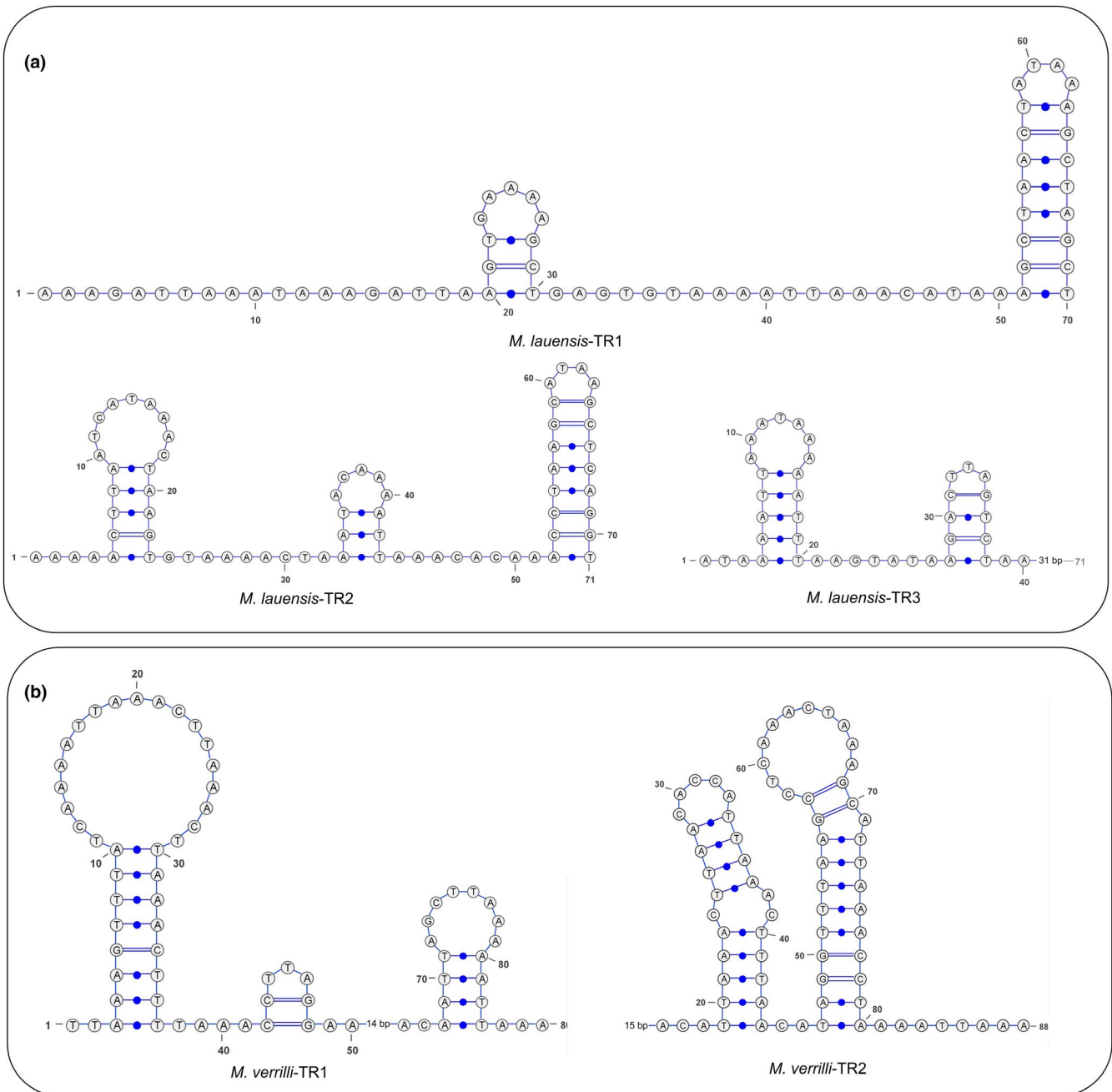
FIGURE 4 Stem-loop structures of the tandem repeat motif in the control region of (a) *Munidopsis lauensis* and (b) *M. verrilli* mitogenomes

relationship with *S. crosnieri* in the gene order tree (Clade I). *K. tyleri* clusters with the *P. haswelli/M. gregaria/N. maculatus* group (Clade II). The Clade III contained all other anomuran species. Our results support that comparisons of mitochondrial gene rearrangements, to some extent, are a useful tool for phylogenetic studies.

Comparative analysis of mitochondrial gene order has been proved to be a valuable phylogenetic tool in crustaceans (Shen, Tsang, Chu, Achituv, & Chan, 2015; Xin et al., 2017). Based on the comparative analysis of mitochondrial gene arrangement within Sessilia, Shen et al. (2015) found that *Amphibalanus amphitrite* (Balanidae) should cluster with *Striatobalanus amaryllis* (Archaeobalanidae) and *Nobia grandis* (Pyrgomatidae) instead of *Megabalanus* (Balanidae), resulting in nonmonophyly of the family Balanidae. Xin et al. (2017) examined the mitochondrial gene arrangements of infraorder Brachyura and suggested that *Clistocoeloma sinensis* may belong to the group Sesarmidae of the superfamily Grapsoidea and that *C. sinensis* and *Sesarmops sinensis* probably belong to sister groups.

3.7 | Phylogenetic analysis

Regardless of different inference methods (BI or ML), the two trees displayed identical topology with high nodal support values (Figure 7). The twelve anomuran species included in this analysis separated into three highly supported clades, one solely comprised of Paguroidea
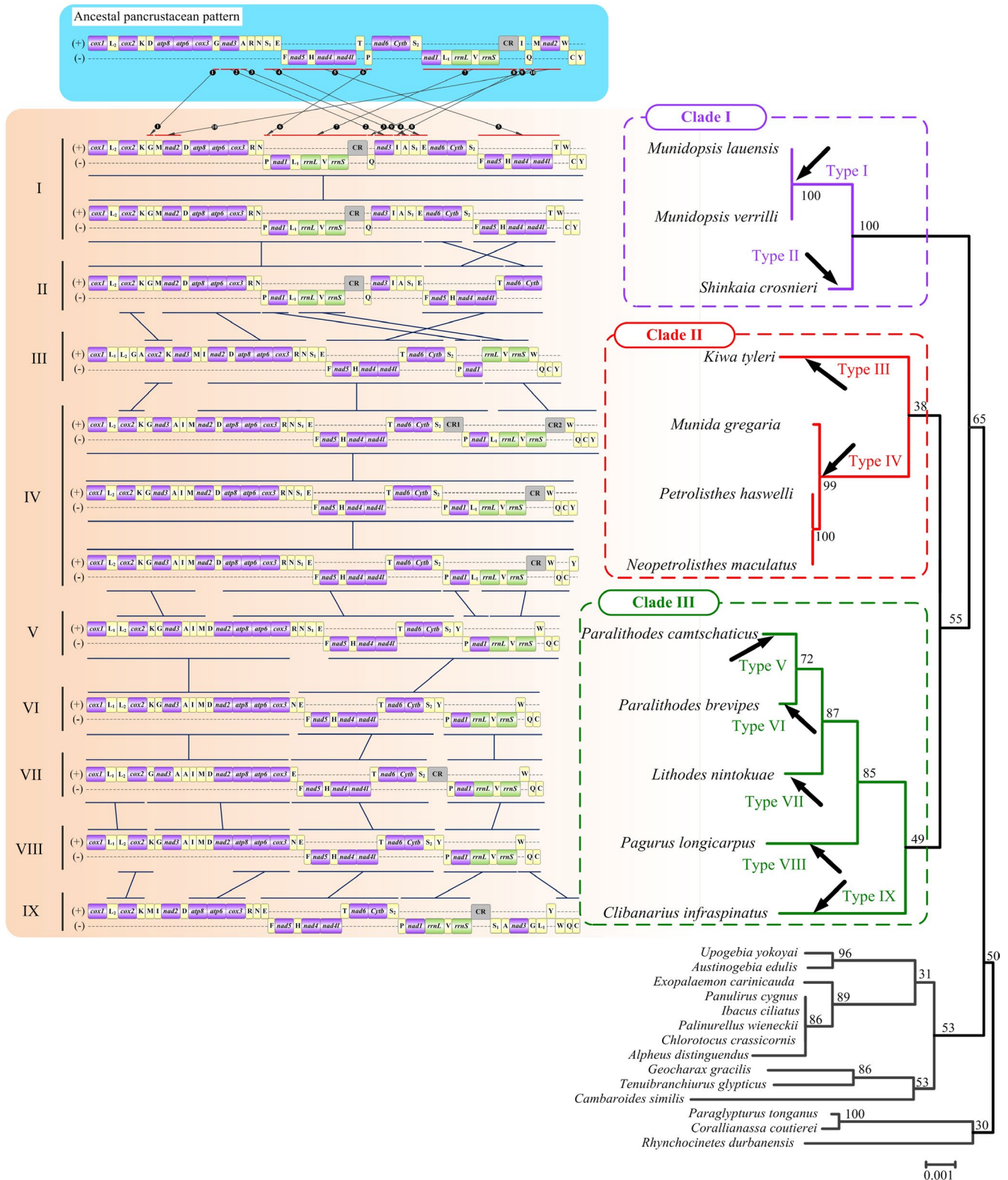
FIGURE 5 Phylogeny reconstructed by gene order, and arrangement of mitochondrial genes in the ancestral pancrustacean pattern and the infraorder Anomura. *Cox1* has been designated the start point for the linear representation of the gene arrangement. All genes are transcribed from left to right. The abbreviations of the genes are the same as Figure 1. The unassigned regions are not presented and gene segments are not drawn to scale. The bars indicate identical gene blocks

	Pan	Pb	Ph	Pl	Pc	Ln	Ci	Kt	Mg	Nm	Sc	Ml	Mv
Pancrustacean	1,326	98	326	134	136	114	130	186	320	326	122	120	120
P. brevipes	98	1,326	582	992	1,184	924	314	460	496	582	150	98	98
P. haswelli	326	582	1,326	546	680	546	216	590	1,188	1,326	230	180	180
P. longicarpus	134	992	546	1,326	1,122	810	162	474	498	546	156	78	78
P. camtschaticus	136	1,184	680	1,122	1,326	924	178	546	586	680	182	116	116
L. nintokuae	114	924	546	810	924	1,326	442	656	546	546	132	82	82
C. infraspinatus	130	314	216	162	178	442	1,326	256	200	216	124	92	92
K. tyleri	186	460	590	474	546	456	256	1,326	546	590	162	106	106
M. gregaria	320	496	1,188	498	586	200	546	546	1,326	1,188	214	164	164
N. maculatus	326	582	1,326	546	680	546	216	590	1,188	1,326	230	180	180
S. crosnieri	122	150	230	156	182	132	124	162	214	230	1,326	678	678
M. lauensis	120	98	180	78	116	82	92	106	164	180	678	1,326	1,326
M. verrilli	120	98	180	78	116	82	92	106	164	180	678	1,326	1,326

FIGURE 6 Pairwise comparisons of mitochondrial gene orders in anomurans obtained from CREx analysis. The numbers indicate the similarities of the compared gene orders, where 1,326 is the highest number and represents identical gene order
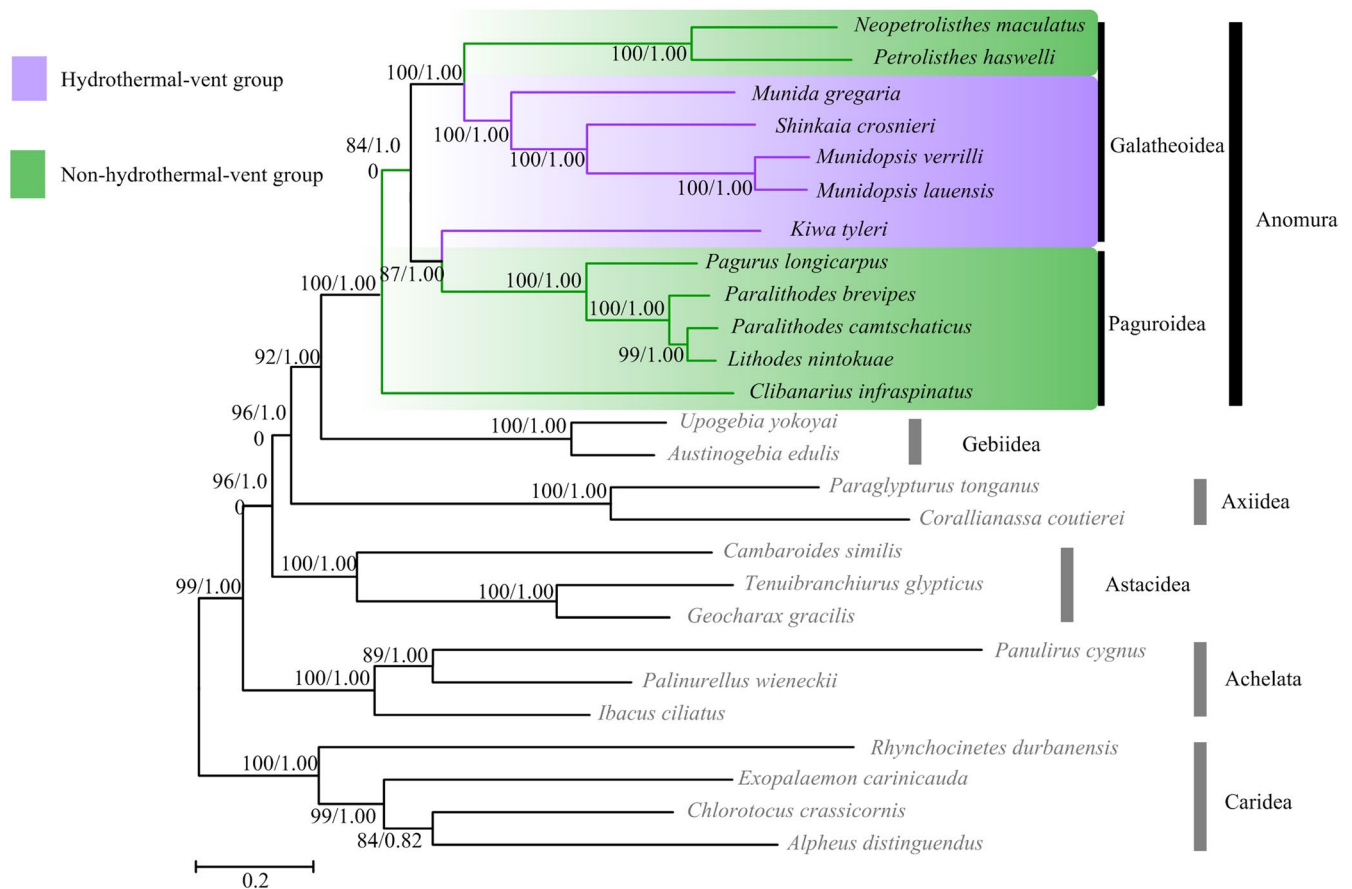

FIGURE 7 Phylogenetic trees derived from maximum likelihood and bayesian analyses based on Anomura mitochondrial PCGs and rRNA sequences with bootstrap values shown on branches. The first number at each node is the bootstrap probability of ML analyses and the second number is Bayesian posterior probability

species, _C. infraspinatus_. The second group consisted of the remaining Paguroidea species and the hydrothermal vent yeti crab _K. tyleri_ from Galatheoidea. Thus, traditional placement of _K. tyleri_ within Galatheoidea based on morphology was not retrieved by our analyses, which is similar to the previous study based on molecular and morphological data (Schnabel et al., 2011). The third group contained all the remaining Galatheoidea species. Thus, the monophyly of the superfamily

Paguroidea and Galatheoidea was not supported. Although the phylogeny of Anomura obtained from nucleotide sequences was inconsistent with that from gene order data, the closest relationship between the hydrothermal vent squat lobsters _M. lauensis_/_M. verrilli_ and _S. crosnieri_ was highly supported in both phylogenies.

Interestingly, the hydrothermal vent galatheid crabs were placed at more evolved positions in the trees. These observations suggested

TABLE 4 Selective pressure analyses of the mitochondrial genes of Anomura lineage

Branch model

Models	LnL	Estimates of parameters	Model compared	2ΔL
Free-ratio model (M1)	−63,224.5337		M1 versus M0	418.2264**
Two-ratio model (M2)	−63,430.4760	$\omega 0 = 0.04065$ $\omega 1 = 0.03082$	M2 versus M0	6.3418
One-ratio model (M0)	−63,433.6469	$\omega = 0.03951$		

Branch-site model

Genes	Models	LnL	Site class	Estimates of parameters				Model compared	2ΔL	Positively selected sites (BEB analysis)
				0	1	2a	2b			
atp8	Model A	−1,308.57	Proportion	0.62298	0.28054	0.06653	0.02996	Model A versus Null model	6.388*	34 E (0.979)
			Background ω	0.0555	1.0000	0.0555	1.0000			
			Foreground ω	0.0555	1.0000	318.2622	318.2622			
	Null model	−1,311.76								
Cytb	Model A	−7,328.57	Proportion	0.9343	0.0269	0.0377	0.0011	Model A versus Null model	0.000	361 W (0.954)
			Background ω	0.0230	1.0000	0.0230	1.0000			
			Foreground ω	0.0230	1.0000	1.0000	1.0000			
	Null model	−7,328.57								
nad3	Model A	−2,405.14	Proportion	0.6570	0.0174	0.3171	0.0084	Model A versus Null model	0.500	15 S (0.997) 29 T (0.969) 32 D (0.997) 36 N (1.000) 38 P (0.997) 47 G (0.993) 72 T (0.993) 79 Y (0.950) 98 F (0.987)
			Background ω	0.0149	1.0000	0.0149	1.0000			
			Foreground ω	0.0149	1.0000	999.0000	999.0000			
	Null model	−2,405.39								
nad4	Model A	−8,916.40	Proportion	0.9056	0.0502	0.0419	0.0023	Model A versus Null model	3.735	83 P (0.998)
			Background ω	0.0209	1.0000	0.0209	1.0000			
			Foreground ω	0.0209	1.0000	35.3398	35.3398			
	Null model	−8,918.26								
nad4l	Model A	−1,949.71	Proportion	0.9023	0.0258	0.0699	0.0020	Model A versus Null model	1.630	43 C (0.970)
			Background ω	0.0225	1.0000	0.0225	1.0000			
			Foreground ω	0.0225	1.0000	57.3451	57.3451			
	Null model	−1,950.52								
nad5	Model A	−12,180.92	Proportion	0.8058	0.0998	0.0841	0.0104	Model A versus Null model	0.015	281 S (0.991) 398 S (0.995) 507 S (0.967)
			Background ω	0.0290	1.0000	0.0290	1.0000			
			Foreground ω	0.0290	1.0000	50.0604	50.0604			
	Null model	−12,180.93								
nad6	Model A	−4,149.03	Proportion	0.7962	0.1152	0.0774	0.0112	Model A versus Null model	9.889**	2 R (0.986) 123 A (0.999)
			Background ω	0.0336	1.0000	0.0336	1.0000			
			Foreground ω	0.0336	1.0000	57.6113	57.6113			
	Null model	−4,153.98								

**$0.001 < p < 0.01$
*$p < 0.001$

that they migrated from hydrothermal vent environments, instead of the remnants of ancient hydrothermal vent species, which support the extinction/repopulation hypothesis (Jacobs & Lindberg, 1998). This invasion event was also found in hydrothermal vent alvinocarid shrimps (Sun, Sha, & Wang, 2018b).

3.8 | Positive selection analysis

In the analysis of branch-specific models, the "two-ratios" (M2) model did not fit the data significantly better than "one-ratio" (M0) model when we set the vent anomurans as a foreground branch ($p > .05$, Table 4). LRTs based on the branch-site models (MA vs. Null model) detected significant signals of positive selection in seven genes (*atp8*, *Cytb*, *nad3*, *nad4*, *nad4l*, *nad5*, and *nad6*) along the hydrothermal vent anomuran branches (Table 4). In total, eighteen positively selected residues were identified by the BEB analyses (BEB value >0.95).

The mitogenome is characterized by its adaptations to the extreme living environments (Castellana, Vicario, & Saccone, 2011). One major adaptation of galatheid squat lobsters is positive selection on mitochondrial genes involved in energy metabolism, hypoxia response, and sulfide-tolerating. NADH dehydrogenase complex (Complex I), acting as a proton pump, is the first and the largest enzyme complex in the respiratory chain (Da Fonseca, Johnson, O'Brien, Ramos, & Antunes, 2008; Mishmar et al., 2003). Cytochrome *b* (Complexes III) use direct coupling for electron transfer and proton translocation (Sazanov, 2015). As part of the regulatory system of complex V (ATP synthase), *atp8* contribute to the proton translocation path and is directly associated with the produce of ATP (Anna et al., 2015; Castellana et al., 2011). These can to some extent explain why more positively selected sites were detected in complexes I, III, and V in our study. Similar results were found in hydrothermal vent alvinocaridid shrimps (Sun, Hui, Wang, et al., 2018; Wang et al., 2017), providing a better understanding of the adaptation of organisms to the deep-sea vent environment.

4 | CONCLUSIONS

In this study, we sequenced and annotated the complete mitogenomes of two squat lobsters *M. lauensis* and *M. verrilli* that colonized hydrothermal vents. Comparative mitogenomic analyses showed that gene content of the two mitogenomes was conserved, whereas gene arrangement displayed diversity. NJ analysis showed the tRNA rearrangements probably arise from tandem duplication and random loss of tRNA genes. CREx analyses reveal the most similarities of mitochondrial gene orders between *M. lauensis*/*M. verrilli* and *S. crosnieri*. The phylogenetic analyses based on both gene order data and nucleotide sequences (PCGs and rRNAs) also indicated that *M. lauensis* and *M. verrilli* were most closely related to *S. crosnieri*. Eighteen positively selected residues in seven genes (*atp8*, *Cytb*, *nad3*, *nad4*, *nad4l*, *nad5*, and *nad6*) were inferred to be positively selected sites for the branch of the

hydrothermal vent anomurans, which may indicate that these genes experienced adaptive evolution.

CONFLICT OF INTEREST

None declared.

AUTHOR CONTRIBUTIONS

Sun S., Sha Z., and Wang Y. designed the manuscript, Sun S. and Sha Z. analyzed the data, and Sun S., Sha Z., and Wang Y. wrote the manuscript.

DATA AVAILABILITY STATEMENT

DNA sequences: Genbank accession number MH717895 for *M. lauensis* and MH717896 for *M. verrilli*.

ORCID

Zhongli Sha (iD) https://orcid.org/0000-0002-2192-3758

REFERENCES

Ahyong, S. T., Schnabel, K. E., & Maas, E. W. (2009). Anomuran phylogeny: New insights from molecular data. In J. W. Martin, K. A. Crandall, & D. L. Felder (Eds.), *Decapod crustacean phylogenetics* (pp. 399–414). Boca Raton, FL: CRC Press.

Akasaki, T., Nikaido, M., Tsuchiya, K., Segawa, S., Hasegawa, M., & Okada, N. (2006). Extensive mitochondrial gene arrangements in coleoid Cephalopoda and their phylogenetic implications. *Molecular Phylogenetics and Evolution*, *38*, 648–658. https://doi.org/10.1016/j.ympev.2005.10.018

Anna, Z., Alexis, R., Schep, D. G., Bason, J. V., Montgomery, M. G., Walker, J. E., … Rubinstein, J. L. (2015). Structure and conformational states of the bovine mitochondrial ATP synthase by cryo-EM. *Elife*, *4*, e10180. https://doi.org/10.7554/elife.10180

Baba, K., Macpherson, E., Poore, G. C. B., Ahyong, T. S., Bermudez, A., Cabezas, P., … Schnabel, E. K. (2008). Catalogue of squat lobsters of the world (Crustacea: Decapoda: Anomura - families Chirostylidae, Galatheidae and Kiwaidae). *Zootaxa*, *1905*, 1–220.

Benson, G. (1999). Tandem repeats finder: A program to analyze DNA sequences. *Nucleic Acids Research*, *27*, 573–580. https://doi.org/10.1093/nar/27.2.573

Bernt, M., Donath, A., Jühling, F., Externbrink, F., Florentz, C., Fritzsch, G., … Stadler, P. F. (2013). MITOS: Improved de novo metazoan mitochondrial genome annotation. *Molecular Phylogenetics and Evolution*, *69*, 313–319. https://doi.org/10.1016/j.ympev.2012.08.023

Bernt, M., Merkle, D., Ramsch, K., Fritzsch, G., Perseke, M., Bernhard, D., … Middendorf, M. (2007). CREx: Inferring genomic rearrangements

based on common intervals. _Bioinformatics_, _23_, 2957–2958. https://doi.org/10.1093/bioinformatics/btm468

Boore, J. L. (1999). Animal mitochondrial genomes. _Nucleic Acids Research_, _27_, 1767–1780. https://doi.org/10.1093/nar/27.8.1767

Boore, J. L., & Brown, W. M. (1998). Big trees from little genomes: Mitochondrial gene order as a phylogenetic tool. _Current Opinion in Genetics & Development_, _8_, 668–674. https://doi.org/10.1016/S0959-437X(98)80035-X

Boore, J. L., Lavrov, D. V., & Brown, W. M. (1998). Gene translocation links insects and crustaceans. _Nature_, _392_, 667–668. https://doi.org/10.1038/33577

Bracken-Grissom, H. D., Cannon, M. E., Cabezas, P., Feldmann, R. M., & Crandall, K. A. (2013). A comprehensive and integrative reconstruction of evolutionary history for anomura (Crustacea: Decapoda). _BMC Evolutionary Biology_, _13_, 128. https://doi.org/10.1186/1471-2148-13-128

Cameron, S. L. (2014). Insect mitochondrial genomics: Implications for evolution and phylogeny. _Annual Review of Entomology_, _59_, 95–117. https://doi.org/10.1146/annurev-ento-011613-162007

Cameron, S. L., Johnson, K. P., & Whiting, M. F. (2007). The mitochondrial genome of the screamer louse _Bothriometopus_ (Phthiraptera: Ischnocera): Effects of extensive gene rearrangements on the evolution of the genome. _Journal of Molecular Evolution_, _65_, 589–604. https://doi.org/10.1007/s00239-007-9042-8

Cameron, S. L., Yoshizawa, K., Mizukoshi, A., Whiting, M. F., & Johnson, K. P. (2011). Mitochondrial genome deletions and minicircles are common in lice (Insecta: Phthiraptera). _BMC Genomics_, _2011_, 12. https://doi.org/10.1186/1471-2164-12-394

Cannicci, S., Schubart, C. D., Innocenti, G., Dahdouh-Guebas, F., Shahdadi, A., & Fratini, S. (2017). A new species of the genus _Parasesarma_ De Man 1895 from East African mangroves and evidence for mitochondrial introgression in sesarmid crabs. _Zoologischer Anzeiger_, _269_, 89–99. https://doi.org/10.1016/j.jcz.2017.08.002

Castellana, S., Vicario, S., & Saccone, C. (2011). Evolutionary patterns of the mitochondrial genome in metazoa: Exploring the role of mutation and selection in mitochondrial protein-coding genes. _Genome Biology and Evolution_, _3_, 1067–1079. https://doi.org/10.1093/gbe/evr040

Chai, H. N., Du, Y. Z., & Zhai, B. P. (2012). Characterization of the complete mitochondrial genomes of _Cnaphalocrocis medinalis_ and _Chilo suppressalis_ (Lepidoptera: Pyralidae). _Journal of Biological Sciences_, _8_, 561–579. https://doi.org/10.7150/ijbs.3540

Chen, S. L., Lee, W., Hottes, A. K., Shapiro, L., & McAdams, H. H. (2004). Codon usage between genomes is constrained by genome-wide mutational processes. _Proceedings of the National Academy of Sciences of the United States of America_, _101_, 3480–3485. https://doi.org/10.1073/pnas.0307827100

Chen, S. C., Wei, D. D., Shao, R., Dou, W., & Wang, J. J. (2014). The complete mitochondrial genome of the booklouse, _Liposcelis decolor_: Insights into gene arrangement and genome organization within the genus _Liposcelis_. _PLoS ONE_, _9_, e91902. https://doi.org/10.1186/1471-2164-15-861

Chen, S. C., Wei, D. D., Shao, R., Shi, J. X., Dou, W., & Wang, J. J. (2014). Evolution of multipartite mitochondrial genomes in the booklice of the genus _Liposcelis_ (Psocoptera). _BMC Genomics_, _15_, 861. https://doi.org/10.1186/1471-2164-15-861

Clement, N. L., Snell, Q., Clement, M. J., Hollenhorst, P. C., Purwar, J., Graves, B. J., … Johnson, W. E. (2010). The GNUMAP algorithm: Unbiased probabilistic mapping of oligonucleotides from next-generation sequencing. _Bioinformatics_, _26_, 38–45. https://doi.org/10.1093/bioinformatics/btp614

Cottin, D., Shillito, B., Chertemps, T., Tanguy, A., Léger, N., & Ravaux, J. (2010). Identification of differentially expressed genes in the hydrothermal vent shrimp _Rimicaris exoculata_ exposed to heat stress. _Marine Genomics_, _3_, 71–78. https://doi.org/10.1016/j.margen.2010.05.002

Da Fonseca, R. R., Johnson, W. E., O'Brien, S. J., Ramos, M. J., & Antunes, A. (2008). The adaptive evolution of the mammalian mitochondrial genome. _BMC Genomics_, _9_, 119. https://doi.org/10.1186/1471-2164-9-119

De Grave, S., Pentcheff, N. D., Ahyong, S. T., Chan, T.-Y., Crandall, K. A., Dworschak, P. C., … Wetzer, R. (2009). A classification of living and fossil genera of decapod Crustaceans. _The Raffles Bulletin of Zoology_, _21_, 1–109.

Dowton, M., & Austin, A. D. (1999). Evolutionary dynamics of a mitochondrial rearrangement "hot spot" in the Hymenoptera. _Molecular Biology and Evolution_, _16_, 298–309. https://doi.org/10.1093/oxfordjournals.molbev.a026111

Drummond, A. J., & Rambaut, A. (2007). BEAST: Bayesian evolutionary analysis by sampling trees. _BMC Evolutionary Biology_, _7_, 214. https://doi.org/10.1186/1471-2148-7-214

Fu, J. Y., Han, B. Y., & Xiao, Q. (2014). Mitochondrial COI and 16sRNA evidence for a single species hypothesis of _E. vitis_, _J. formosana_ and _E. onukii_ in East Asia. _PLoS ONE_, _9_, e115259. https://doi.org/10.1371/journal.pone.0115259

Gissi, C., Iannelli, F., & Pesole, G. (2008). Evolution of the mitochondrial genome of Metazoa as exemplified by comparison of congeneric species. _Heredity_, _101_, 301–320. https://doi.org/10.1038/hdy.2008.62

Gu, J., Guo, R., Yan, K., Lei, J., Gao, N., & Yang, M. (2016). The arquitecture of the mammalian respirasome. _Nature_, _537_, 639–644. https://doi.org/10.1038/nature19359

Hao, J., Sun, Q., Zhao, H., Sun, X., Gai, Y., & Yang, Q. (2012). The complete mitochondrial genome of _Ctenoptilum vasava_ (Lepidoptera: Hesperiidae: Pyrginae) and its phylogenetic implication. _Comparative & Functional Genomics_, _328049_, 1–13. https://doi.org/10.1155/2012/328049

Hassanin, A., Léger, N., & Deutsch, J. (2005). Evidence for multiple reversals of asymmetric mutational constraints during the evolution of the mitochondrial genome of Metazoa, and consequences for phylogenetic inferences. _Systematic Biology_, _54_, 277–298. https://doi.org/10.1080/10635150590947843

Hu, F., Lin, Y., & Tang, J. (2014). MLGO: Phylogeny reconstruction and ancestral inference from gene-order data. _BMC Bioinformatics_, _15_, 354. https://doi.org/10.1186/s12859-014-0354-6

Hui, M., Cheng, J., & Sha, Z. (2018). Adaptation to the deep-sea hydrothermal vents and cold seeps: Insights from the transcriptomes of _Alvinocaris longirostris_, in both environments. _Deep Sea Research Part I: Oceanographic Research Papers_, _135_, 23–33. https://doi.org/10.1016/j.dsr.2018.03.014

Hui, M., Song, C., Liu, Y., Li, C., & Cui, Z. (2017). Exploring the molecular basis of adaptive evolution in hydrothermal vent crab _Austinograea alayseae_ by transcriptome analysis. _PLoS ONE_, _12_, e0178417. https://doi.org/10.1371/journal.pone.0178417

Hung, C. M., Lin, R. C., Chu, J. H., Yeh, C. F., Yao, C. J., & Li, S. H. (2013). The de novo assembly of mitochondrial genomes of the extinct passenger pigeon (_Ectopistes migratorius_) with next generation sequencing. _PLoS ONE_, _8_, e56301. https://doi.org/10.1371/journal.pone.0056301

Ivey, J. L., & Santos, S. R. (2007). The complete mitochondrial genome of the hawaiian anchialine shrimp _Halocaridina rubra_, Holthuis, 1963 (Crustacea: Decapoda: Atyidae). _Gene_, _394_, 35–44. https://doi.org/10.1016/j.gene.2007.01.009

Jacobs, D. K., & Lindberg, D. R. (1998). Oxygen and evolutionary patterns in the sea: Onshore/offshore trends and recent recruitment of deep-sea faunas. _Proceedings of the National Academy of Sciences of the United States of America_, _95_, 9396–9401. https://doi.org/10.1073/pnas.95.16.9396

Kanmiya, K., Ueda, S., Kasai, A., Yamashita, K., Sato, Y., & Yoshiyasu, Y. (2011). Proposal of new specific status for tea-infesting populations of the nominal citrus spiny whitefly _Aleurocanthus spiniferus_ (Homoptera: Aleyrodidae). _Zootaxa_, _2797_, 25–44.

Ki, J. S., Park, H. G., & Lee, J. S. (2009). The complete mitochondrial genome of the cyclopoid copepod *Paracyclopina nana*: A highly divergent genome with novel gene order and atypical gene numbers. *Gene*, *435*, 13–22. https://doi.org/10.1016/j.gene.2009.01.005

Kim, M. I., Baek, J. Y., Kim, M. J., Jeong, H. C., Kim, K. G., Bae, C. H., ... Kim, I. (2009). Complete nucleotide sequence and organization of the mitogenome of the red-spotted apollo butterfly, *Parnassius bremeri* (Lepidoptera: Papilionidae) and comparison with other lepidopteran insects. *Molecules and Cells*, *28*, 347–363. https://doi.org/10.1007/s10059-009-0129-5

Kim, S., Choi, H. G., Park, J. K., & Min, G. S. (2013). The complete mitochondrial genome of the subarctic red king crab, *Paralithodes camtschaticus* (Decapoda, Anomura). *Mitochondrial DNA*, *24*, 350–352. https://doi.org/10.3109/19401736.2012.760555

Korkmaz, E. M., Aydemir, H. B., Temel, B., Budak, M., & Başıbüyük, H. H. (2017). Mitogenome evolution in cephini (Hymenoptera: Cephidae): Evidence for parallel adaptive evolution. *Biochemical Systematics and Ecology*, *71*, 137–146. https://doi.org/10.1016/j.bse.2017.02.004

Lanfear, R., Calcott, B., Ho, S. Y., & Guindon, S. (2012). PartitionFinder: Combined selection of partitioning schemes and substitution models for phylogenetic analyses. *Molecular Biology and Evolution*, *29*, 1695–1701. https://doi.org/10.1093/molbev/mss020

Laslett, D., & Canback, B. (2008). ARWEN: A program to detect tRNA genes in metazoan mitochondrial nucleotide sequences. *Bioinformatics*, *24*, 172–175. https://doi.org/10.1093/bioinformatics/btm573

Levinson, G., & Gutman, G. A. (1987). Slipped-strand mispairing: A major mechanism for DNA sequence evolution. *Molecular Biology and Evolution*, *4*, 203–221. https://doi.org/10.1093/oxfordjournals.molbev.a040442

Li, R., Zhu, H., Ruan, J., Qian, W., Fang, X., Shi, Z., ... Wang, J. (2010). De novo assembly of human genomes with massively parallel short read sequencing. *Genome Research*, *20*, 265–272. https://doi.org/10.1101/gr.097261.109

Librado, P., & Rozas, J. (2009). DnaSP v5: A software for comprehensive analysis of DNA polymorphism data. *Bioinformatics*, *25*, 1451–1452. https://doi.org/10.1093/bioinformatics/btp187

Little, C. T. S., & Vrijenhoek, R. C. (2003). Are hydrothermal vent animals living fossils? *Trends in Ecology & Evolution*, *18*, 582–588. https://doi.org/10.1016/j.tree.2003.08.009

Luo, Y., Yang, X., & Gao, Y. (2013). Mitochondrial DNA response to high altitude: A new perspective on high-altitude adaptation. *Mitochondrial DNA*, *24*, 313–319. https://doi.org/10.3109/19401736.2012.760558

Machida, R. J., Miya, M. U., Nishida, M., & Nishida, S. (2002). Complete mitochondrial DNA sequence of *Tigriopus japonicus* (Crustacea: Copepoda). *Marine Biotechnology*, *4*, 406–417. https://doi.org/10.1007/s10126-002-0033-x

Martin, J. W., & Haney, T. A. (2005). Decapod crustaceans from hydrothermal vents and cold seeps: A review through 2005. *Zoological Journal of the Linnean Society*, *145*, 445–522. https://doi.org/10.1111/j.1096-3642.2005.00178.x

Mishmar, D., Ruiz-Pesini, E., Golik, P., Macaulay, V., Clark, A. G., Hosseini, S., ... Brown, M. D. (2003). Natural selection shaped regional mtDNA variation in humans. *Proceedings of the National Academy of Sciences of the United States of America*, *100*, 171–176. https://doi.org/10.1073/pnas.0136972100

Ojala, D., Montoya, J., & Attardi, G. (1981). TRNA punctuation model of RNA processing in human mitochondrial. *Nature*, *290*, 470–474. https://doi.org/10.1038/290470a0

Perna, N. T., & Kocher, T. D. (1995). Patterns of nucleotide composition at fourfold degenerate sites of animal mitochondrial genomes. *Journal of Molecular Evolution*, *41*, 353–358. https://doi.org/10.1007/BF01215182

Plotkin, J. B., & Kudla, G. (2011). Synonymous but not the same: The causes and consequences of codon bias. *Nature Reviews Genetics*, *12*, 32–42. https://doi.org/10.1038/nrg2899

Ronquist, F., & Huelsenbeck, J. P. (2003). MrBayes 3: Bayesian phylogenetic inference undermixed models. *Bioinformatics*, *19*, 1572–1574. https://doi.org/10.1093/bioinformatics/btg180

Salvato, P., Simonato, M., Battisti, A., & Negrisolo, E. (2008). The complete mitochondrial genome of the bag-shelter moth *Ochrogaster lunifer* (Lepidoptera, Notodontidae). *BMC Genomics*, *9*, 331. https://doi.org/10.1186/1471-2164-9-331

Sazanov, L. A. (2015). A giant molecular proton pump: Structure and mechanism of respiratory complex I. *Nature Reviews Molecular Cell Biology*, *16*, 375–388. https://doi.org/10.1038/nrm3997

Schnabel, K. E., Ahyong, S. T., & Maas, E. W. (2011). Galatheoidea are not monophyletic – molecular and morphological phylogeny of the squat lobsters (Decapoda: Anomura) with recognition of a new superfamily. *Molecular Phylogenetics and Evolution*, *58*, 157–168. https://doi.org/10.1016/j.ympev.2010.11.011

Scott, G. R., Schulte, P. M., Egginton, S., Scott, A. L. M., Richards, J. G., & Milsom, W. K. (2011). Molecular evolution of cytochrome *c* oxidase underlies high-altitude adaptation in the bar-headed goose. *Molecular Biology and Evolution*, *28*, 351–363. https://doi.org/10.1093/molbev/msq205

Shao, R., Barker, S. C., Li, H., Song, S., Poudel, S., & Su, Y. (2015). Fragmented mitochondrial genomes in two suborders of parasitic lice of eutherian mammals (Anoplura and Rhynchophthirina, Insecta). *Scientific Reports*, *5*, 17389. https://doi.org/10.1038/srep17389

Shao, R., Zhu, X. Q., Barker, S. C., & Herd, K. (2012). Evolution of extensively fragmented mitochondrial genomes in the lice of humans. *Genome Biology and Evolution*, *4*, 1088–1101. https://doi.org/10.1093/gbe/evs088

Shen, X., Tsang, L. M., Chu, K. H., Achituv, Y., & Chan, B. K. K. (2015). Mitochondrial genome of the intertidal acorn barnacle Tetraclita serrata Darwin, 1854 (Crustacea: Sessilia): Gene order comparison and phylogenetic consideration within Sessilia. *Marine Genomics*, *22*, 63–69. https://doi.org/10.1016/j.margen.2015.04.004

Simon, C., Buckley, T. R., Frati, F., Stewart, J. B., & Beckenbach, A. T. (2006). Incorporating molecular evolution into phylogenetic analysis, and a new compilation of conserved polymerase chain reaction primers for animal mitochondrial DNA. *Annual Review of Ecology Evolution and Systematics*, *37*, 545–579. https://doi.org/10.1146/annurev.ecolsys.37.091305.110018

Smith, M. J., Arndt, A., Gorski, S., & Fajber, E. (1993). The phylogeny of echinoderm classes based on mitochondrial gene arrangements. *Journal of Molecular Evolution*, *36*, 545–554. https://doi.org/10.1007/BF00556359

Stamatakis, A., Hoover, P., & Rougemont, J. (2008). A rapid bootstrap algorithm for the RAxML web servers. *Systematic Biology*, *57*, 758–771. https://doi.org/10.1080/10635150802429642

Stanton, D. J., Daehler, L. L., Moritz, C. C., & Brown, W. M. (1994). Sequences with the potential to form stem-and-loop structures are associated with coding-region duplications in animal mitochondrial DNA. *Genetics*, *137*, 233–241.

Stothard, P., & Wishart, D. S. (2005). Circular genome visualization and exploration using CGView. *Bioinformatics*, *21*, 537–539. https://doi.org/10.1093/bioinformatics/bti054

Sun, S., Hui, M., Wang, M., & Sha, Z. (2018). The complete mitochondrial genome of the alvinocaridid shrimp *Shinkaicaris leurokolos* (Decapoda, Caridea): Insight into the mitochondrial genetic basis of deep-sea hydrothermal vent adaptation in the shrimp. *Comparative Biochemistry and Physiology Part D: Genomics and Proteomics*, *25*, 42–52. https://doi.org/10.1016/j.cbd.2017.11.002

Sun, S., Sha, Z., & Wang, Y. (2018a). Complete mitochondrial genome of the first deep-sea spongicolid shrimp *Spongiocaris panglao* (Decapoda: Stenopodidea): Novel gene arrangement and the phylogenetic position and origin of stenopodidea. *Gene*, *676*, 123–138. https://doi.org/10.1016/j.gene.2018.07.026

Sun, S., Sha, Z., & Wang, Y. (2018b). Phylogenetic position of Alvinocarididae (Crustacea: Decapoda: Caridea): New insights into the origin and evolutionary history of the hydrothermal vent alvinocarid shrimps. *Deep-Sea Research Part I*, *141*, 93–105. https://doi.org/10.1016/j.dsr.2018.10.001

Taanman, J. W. (1999). The mitochondrial genome: Structure, transcription, translation and replication. *Biochimica Et Biophysica Acta*, *1410*, 103–123. https://doi.org/10.1016/S0005-2728(98)00161-3

Talavera, G., & Castresana, J. (2007). Improvement of phylogenies after removing divergent and ambiguously aligned blocks from protein sequence alignments. *Systematic Biology*, *56*, 564–577. https://doi.org/10.1080/10635150701472164

Tamura, K., Peterson, D., Peterson, N., Stecher, G., Nei, M., & Kumar, S. (2011). MEGA5: Molecular evolutionary genetics analysis using maximum likelihood, evolutionary distance, and maximum parsimony methods. *Molecular Biology and Evolution*, *28*, 2731–2739. https://doi.org/10.1093/molbev/msr121

Wang, X., & Lavrov, D. V. (2011). Gene recruitment-A common mechanism in the evolution of transfer rna gene families. *Gene*, *475*, 22–29. https://doi.org/10.1016/j.gene.2010.12.009

Wang, Y., Shen, Y. J., Feng, C. G., Zhao, K., Song, Z. B., Zhang, Y. P., … He, S. P. (2016). Mitogenomic perspectives on the origin of Tibetan loaches and their adaptation to high altitude. *Scientific Reports*, *6*, 29690. https://doi.org/10.1038/srep29690

Wang, Z., Shi, X., Sun, L., Bai, Y., Zhang, D., & Tang, B. (2017). Evolution of mitochondrial energy metabolism genes associated with hydrothermal vent adaption of alvinocaridid shrimps. *Genes and Genomics*, *39*, 1367–1376. https://doi.org/10.1007/s13258-017-0600-1

Wei, D. D., Yuan, M. L., Wang, B. J., Zhou, A. W., Dou, W., & Wang, J. J. (2012). Population genetics of two asexually and sexually reproducing psocids species inferred by the analysis of mitochondrial and nuclear DNA sequences. *PLoS ONE*, *7*, e33883. https://doi.org/10.1371/journal.pone.0033883

Wilkinson, G. S., & Chapman, A. M. (1991). Length and sequence variation in evening bat D loop mtDNA. *Genetics*, *128*, 607–617. https://doi.org/10.1101/gad.5.7.1309

Wu, M., Gu, J., Guo, R., Huang, Y., & Yang, M. (2016). Structure of mammalian respiratory supercomplex I1III2IV1. *Cell*, *167*, 1598–1609. https://doi.org/10.1016/j.cell.2016.11.012

Xin, Z. Z., Liu, Y., Zhang, D. Z., Chai, X. Y., Wang, Z. F., Zhang, H. B., … Liu, Q. N. (2017). Complete mitochondrial genome of *Clistocoeloma sinensis* (Brachyura: Grapsoidea): Gene rearrangements and higher-level phylogeny of the Brachyura. *Scientific Reports*, *7*, 4128. https://doi.org/10.1038/s41598-017-04489-9

Yang, J. S., Lu, B., Chen, D. F., Yu, Y. Q., Yang, F., Nagasawa, H., … Yang, W. J. (2013). When did decapods invade hydrothermal vents? Clues from the western pacific and indian oceans. *Molecular Biology and Evolution*, *30*, 305–309. https://doi.org/10.1093/molbev/mss224

Yang, J. S., & Yang, W. J. (2008). The complete mitochondrial genome sequence of the hydrothermal vent galatheid crab *Shinkaia crosnieri* (Crustacea: Decapoda: Anomura): A novel arrangement and incomplete tRNA suite. *BMC Genomics*, *9*, 257. https://doi.org/10.1186/1471-2164-9-257

Yang, J., Ye, F., & Huang, Y. (2016). Mitochondrial genomes of four katydids (Orthoptera: Phaneropteridae): New gene rearrangements and their phylogenetic implications. *Gene*, *575*, 702–711. https://doi.org/10.1016/j.gene.2015.09.052

Yang, Z. (2007). PAML4: Phylogenetic analysis by maximum likelihood. *Molecular Biology and Evolution*, *24*, 1586–1591. https://doi.org/10.1093/molbev/msm088

Yang, Z., Wong, W. S. W., & Nielsen, R. (2005). Bayes empirical bayes inference of amino acid sites under positive selection. *Molecular Biology and Evolution*, *22*, 1107–1118. https://doi.org/10.1093/molbev/msi097

Yu, L., Wang, X., Ting, N., & Zhang, Y. (2011). Mitogenomic analysis of Chinese snub-nosed monkeys: Evidence of positive selection in NADH dehydrogenase genes in high-altitude adaptation. *Mitochondrion*, *11*, 497–503. https://doi.org/10.1016/j.mito.2011.01.004

Yuan, M. L., Zhang, Q. L., Zhang, L., Jia, C. L., Li, X. P., Yang, X. Z., & Feng, R. Q. (2018). Mitochondrial phylogeny, divergence history and high-altitude adaptation of grassland caterpillars (Lepidoptera: Lymantriinae: *Gynaephora*) inhabiting the tibetan plateau. *Molecular Phylogenetics and Evolution*, *122*, 116–124. https://doi.org/10.1016/j.ympev.2018.01.016

Yuan, Y., Li, Q., Yu, H., & Kong, L. (2012). The complete mitochondrial genomes of six heterodont bivalves (Tellinoidea and Solenoidea): Variable gene arrangements and phylogenetic implications. *PLoS ONE*, *7*, e32353. https://doi.org/10.1371/journal.pone.0032353

Zhang, B., Zhang, Y. H., Wang, X., Zhang, H. X., & Lin, Q. (2017). The mitochondrial genome of a sea anemone *Bolocera* sp. exhibits novel genetic structures potentially involved in adaptation to the deep-sea environment. *Ecology and Evolution*, *7*, 4951–4962. https://doi.org/10.1002/ece3.3067

Zhang, G. H., Yuan, Z. J., Zhang, C. X., Yin, K. S., Tang, M. J., Guo, H. W., … Xiao, Q. (2014). Detecting deep divergence in seventeen populations of tea geometrid (*Ectropis obliqua* Prout) in China by COI mtDNA and cross-breeding. *PLoS ONE*, *9*, e99373. https://doi.org/10.1371/journal.pone.0099373

Zhang, J., Sun, Q. L., Luan, Z. D., Lian, C., & Sun, L. (2017). Comparative transcriptome analysis of Rimicaris sp. reveals novel molecular features associated with survival in deep-sea hydrothermal vent. *Scientific Reports*, *7*, 2000. https://doi.org/10.1038/s41598-017-02073-9

Zhang, Q. L., Zhang, L., Zhao, T. X., Wang, J., Zhu, Q. H., Chen, J. Y., & Yuan, M. L. (2017). Gene sequence variations and expression patterns of mitochondrial genes are associated with the adaptive evolution of two Gynaephora species (Lepidoptera: Lymantriinae) living in different high-elevation environments. *Gene*, *610*, 148–155. https://doi.org/10.1016/j.gene.2017.02.014

Zhou, L., Lin, Y., Feng, B., Zhao, J., & Tang, J. (2017). Phylogeny analysis from gene-order data with massive duplications. *BMC Genomics*, *18*, 13–20. https://doi.org/10.1186/s12864-017-4129-0

Zhou, T., Shen, X., Irwin, D. M., Shen, Y., & Zhang, Y. (2014). Mitogenomic analyses propose positive selection in mitochondrial genes for high-altitude adaptation in galliform birds. *Mitochondrion*, *18*, 70–75. https://doi.org/10.1016/j.mito.2014.07.012

Zuker, M. (2003). Mfold web server for nucleic acid folding and hybridization prediction. *Nucleic Acids Research*, *31*, 3406–3415. https://doi.org/10.1093/nar/gkg595

SUPPORTING INFORMATION

Additional supporting information may be found online in the Supporting Information section at the end of the article.

How to cite this article: Sun S, Sha Z, Wang Y. The complete mitochondrial genomes of two vent squat lobsters, *Munidopsis lauensis* and *M. verrilli*: Novel gene arrangements and phylogenetic implications. *Ecol Evol*. 2019;9: 12390–12407. https://doi.org/10.1002/ece3.5542